Ancient TL

www.ancienttl.org · ISSN: 2693-0935

Issue 38(2) - December 2020
https://doi.org/10.26034/la.atl.v38.i2

ISSN 2693-0935

Ancient TL

A periodical devoted to Luminescence and ESR dating

Department of Physics, East Carolina University, 1000 East 5th Street, Greenville, NC 27858, USA

http://ancienttl.org

December 2020, Volume 38 No.2

Ancient TL

Started by the late David Zimmerman in 1977

Ancient TL

'gamma': An R Package for Dose Rate Estimation from In-Situ Gamma-Ray Spectrometry Measurements

Brice Lebrun,[1*] Nicolas Frerebeau,[1] Guilhem Paradol[2], Guillaume Guérin,[1] Norbert Mercier,[1] Chantal Tribolo,[1] Christelle Lahaye,[1] Magali Rizza[3]

[1] IRAMAT-CRP2A, UMR 5060, CNRS - Université Bordeaux Montaigne, France
[2] SyMMES, UMR 5819 - CEA, CNRS, Université Grenoble Alpes, France
[3] CEREGE, Aix Marseille Univ, CNRS, IRD, INRAE, Coll France

*Corresponding Author: brice.lebrun@u-bordeau-montaigne.fr

Received: September 25, 2020; in final form: October 28, 2020

Abstract

***In situ* gamma spectrometry is a useful technique used by the Luminescence and ESR dating community to improve the representativity of dose rate measurements in the context of gamma dose rate heterogeneities around dated material. This paper presents 'gamma', a new R package and its graphical user interface 'gammaShiny', allowing a reliable and reproducible workflow for *in situ* gamma spectrometry data analysis in the context of luminescence and ESR dating.**

Keywords: Archaeology, Geochronology, Luminescence dating, Gamma spectrometry

1. Introduction

In situ gamma spectrometry is a powerful tool used in luminescence dating to tackle gamma dose rate heterogeneity (Aitken, 1998; Klusoň, 2010). A gamma spectrometer probe records gamma rays emitted within a sphere of radius equal to 30 – 50 cm (Figure 1 in Guérin & Mercier, 2011) whereas a classic BeGe laboratory gamma spectrometer with planar or coaxial geometry only characterizes samples of a few dozen cubic centimeters,thus greatly improving the representativity of the measurement (Gilmore, 2008).

Different techniques are currently used in luminescence and ESR dating field to determine the gamma dose rate from *in situ* gamma spectrometry measurements:

- The 'window technique', that consists in selecting different parts of the spectra to quantify the U and Th-series and K radioelements contents in the sediment, around the probe.
- The 'threshold techniques', that allow a direct determination of the gamma dose rate without individual determination of K, U and Th series radioelements. Murray et al. (1978) have shown that the gamma dose rate can be estimated using the proportionality existing between the number of counts measured above a certain energy and the gamma dose rate. Mercier & Falguères (2007) developed this approach for a NaI(Tl) probe. They conclude that the measurement time (and consequently the risk of changing temperature during the measurement) is significantly reduced in comparison with the 'window technique'.

There are two methods based on the 'threshold technique': in counts and in energy. In both cases, Guérin & Mercier (2011) have shown that the environmental gamma dose rate determined in this way does not depend on water presence, nor on U-series disequilibrium. They have also shown few dependence on the gamma dose rate with the nature of the sediment.

The majority of *in situ* gamma-ray spectrometers produce energy shifted and spectrally distorted spectra. This could be due to the fact that detector crystals (usually LaBr or NaI) are often used in unstable temperature conditions (Casanovas et al., 2012). As a result, spectrum processing is required before conversion from a spectrum to gamma dose rate.

A typical workflow for energy shifting correction requires manual identification of reference peaks. This is usually

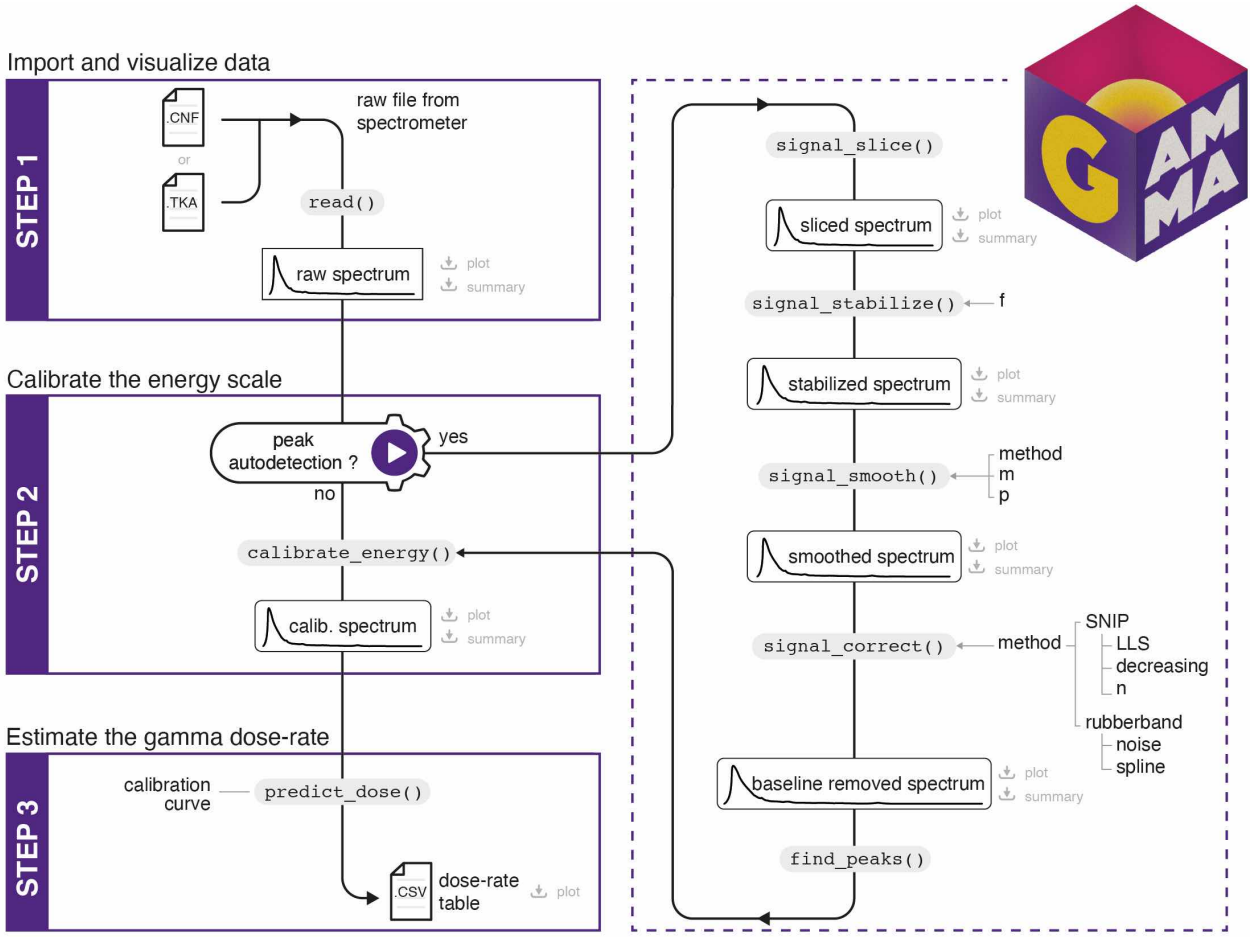

Figure 1. A typical workflow within the 'gamma' package.

performed using proprietary software such as Genie2000® (Canberra division of Mirion technologies, Windows OS only). Once reference peaks are identified, a new channel-energy curve is generated, taking into account the apparent shift between the observed and theoretical energies of these peaks. To this day, there is no turnkey solution for these steps and personal or laboratory-based solutions are implemented, e.g. Visual Basic Advance® macros within Microsoft Excel®.

There are two challenging issues to these existing approaches. The first one is the lack of transparency: details of spectrum processing are not presented in the publications and researcher's internally developed solutions are not made available to the community, greatly limiting reproducibility and reliability of the measurements (see Kreutzer et al., 2017 for a broader discussion in the field of luminescence dating). Secondly, the use of proprietary software limits their access by the community, hindering their maintenance and evolution.

To address theses differents issues, we present an integrated solution to analyse *in situ* gamma spectrometry data, from raw spectrum processing to gamma dose-rate estimation: the **R** package 'gamma'. The **R** programming language (R Core Team, 2020) has many advantages, starting with its ease of learning and use. R is available on all computer platforms and its community offers efficient support. R is distributed under the GNU General Public License (therefore free of charge), ensuring transparency and modularity. Finally, several **R** packages dedicated to geochronology already exist (such as the 'Luminescence' package; Kreutzer et al., 2012).

2. The R package 'gamma'

The 'gamma' package allows the user to import, inspect and correct the energy scale of one or multiple spectra. It provides methods for estimating the gamma dose rate by the use of built-in or custom calibration curves. A graphical user interface (GUI) is also provided through the dedicated **R** package 'gammaShiny', using the 'shiny' package (Chang et al., 2020).

2.1. Workflow overview

This section present a typical workflow within the 'gamma' package (Figure 1). A walk-through guide is also provided in the package manual. The following examples can be reproduced in any integrated development environ-

ment (like RStudio^{TM} Desktop; http://rstudio.org) or in the **R** terminal.

Once the 'gamma' package is loaded with `library(gamma)`, processing a spectrum is achieved in three steps: import, energy calibration and dose-rate estimation which are detailed hereafter.

All of these steps can be performed through the GUI, which can be launched with `launch_app()` after loading the package with `library(gammaShiny)`. Note that we chose to develop a GUI to allow the use of 'gamma' for users who might not feel comfortable with the use of the command line. However, only the full publication of scripts along with the results guarantees the reproducibility of published studies.

2.1.1 Step 1: import and inspect a gamma spectrum

The 'gamma' package supports the most common type of spectrum files: Canberra CAM (.CNF) and Programmers Toolkit files (.TKA). This prevents spending time on data transformation and preserves file metadata. The `read()` function allows to import a CNF-file with the path of the file as a single argument. When the path leads to a directory instead of a single file, all spectra included in the directory are imported.

```
## Get an example file
cnf <- system.file(
  "extdata/LaBr.CNF",
  package = "gamma"
)
## Import data
spc <- read(cnf)
spc
```

Spectra are stored as instances of an S4 class. Many mutator methods and group generic functions are available for basic operations and data wrangling. The `plot(spc)` method allows to quickly graphically inspect the data.

2.1.2 Step 2: adjust the energy scale

The energy calibration of a spectrum is a challenging part and must be performed before dose rate estimation. The solution presented here requires the user to specify the position (channel) of at least three observed peaks and their corresponding theoretical energies (in keV). A second order polynomial model is fitted on these energy *versus* channel values, then used to predict the new energy scale of the spectrum.

The package allows the user to provide the channel-energy pairs to be used. However, the spectrum can be noisy so it is difficult to properly identify the peak channel. In this case, a better approach may be to pre-process the spectrum (variance-stabilization, smoothing and baseline correction) and perform a peak detection (Figure 2). Once the peak detection is satisfactory, the user can set the corresponding energy values (in keV) and use these lines to calibrate the energy scale of the spectrum. All signal processing methods are prefixed with `signal_`.

Cleaning Several channels can be dropped to retain only part of the spectrum with `signal_slice()`. If no specific value is provided, an attempt is made to define the number of channels to skip at the beginning of the spectrum. This drops all channels before the highest count maximum. This is intended to deal with the artefact produced by the rapid growth of random background noise towards low energies.

Stabilization The stabilization step aims at improving the identification of peaks with a low signal-to-noise ratio. This particularly targets higher energy peaks. To perform this step, a function is applied to all the intensity values of the spectrum with `signal_stabilize()`. The example below uses a square root transformation but any user defined function can be used.

Smoothing Counting artefacts can be removed by smoothing intensities with `signal_smooth()`. Several methods are implemented here such as (weighted) sliding-average and Savitzky-Golay filter (Savitzky & Golay, 1964; Gorry, 1990). The example below uses the Savitzky-Golay filter as this method usually provides better results, at the expense of a longer computing time.

Baseline correction Spectrum baseline can be estimated and removed with `signal_correct()` using specialized SNIP algorithm (Ryan et al., 1988; Morháč et al., 1997; Morháč & Matoušek, 2008).

Peak detection `find_peaks()` allows automatic peak position detection on a baseline-corrected spectrum. For a successful detection, a local maximum has to be the highest one in a given window and has to be higher than k times the noise (estimated as the Median Absolute Deviation) to be recognized as a peak.

Energy calibration The energy scale calibration needs the energy values of detected peaks to be set. `calibrate_energy()` then fits a second order polynomial model to predict the new spectrum energy scale.

```
library(magrittr)
## Signal processing
tmp <- spc %>%
  signal_slice() %>%
  signal_stabilize(f = sqrt) %>%
  signal_smooth(method = "savitzky", m = 21)
      ↪ %>%
  signal_correct(method = "SNIP")
## Peak detection
pks <- peaks_find(tmp)
set_energy(pks) <- c(238, NA, NA, NA,
                     1461, NA, NA, 2615)
## Energy scale calibration
spc2 <- energy_calibrate(spc, pks)
```

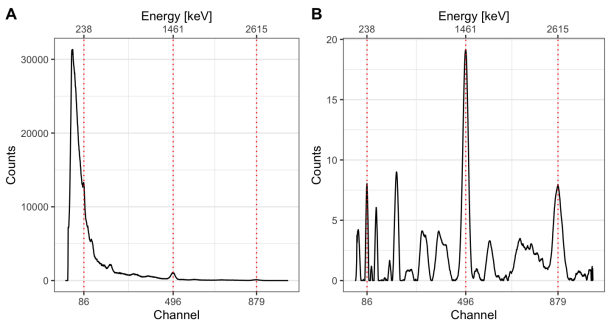

Figure 2. (A) Raw gamma ray spectrum from in situ measurement; (B) Processed spectrum used for peak finding along with the detected peaks.

2.1.3 Step 3: gamma dose-rate estimation

To estimate the gamma dose rate, one of the calibration curves distributed with this package can be used (Figure 3). These built-in curves are in use in several luminescence dating laboratories and can be used to replicate published results. As these curves are instrument specific, the user may have to build its own curve. The ‘gamma’ package provides a set of functions to build custom calibration curves.

```
## Load the calibration curve
data("BDX_LaBr_1", package = "gamma")
## Estimate the gamma dose rate
doses <- dose_predict(BDX_LaBr_1, spc2)
doses
```

The construction of a calibration curve with `dose_fit()` requires a set of reference spectra for which the gamma dose rate is known (see Miallier et al., 2009 for the reference values in use at the CRP2A laboratory) and a background noise measurement. First, each reference spectrum is integrated over a given interval, then normalized to active time and corrected for background noise. The dose rate is finally modelled by the integrated signal value used as a linear predictor (York et al., 2004). `dose_predict()` returns the predicted dose rate value with both the count and energy threshold approaches.

3. Discussion

The ‘gamma’ package provides a convenient and reproducible toolkit for *in situ* gamma spectrometry data analysis. Along with the dedicated ’gammaShiny’ package (GUI), it offers a useful set of functions for spectra processing, calibration curve building and dose rate estimation.

The ‘gamma’ package allows batch processing of spectra. To ensure the reliability of the produced results, manual verification is strongly recommended since automatic detection may sometime produce unreliable results, especially when the processed spectra display poor signal-to-noise ratios. In the future, improvement of the automatic peak detection process is to be expected (Guilhem Paradol, pers. comm.).

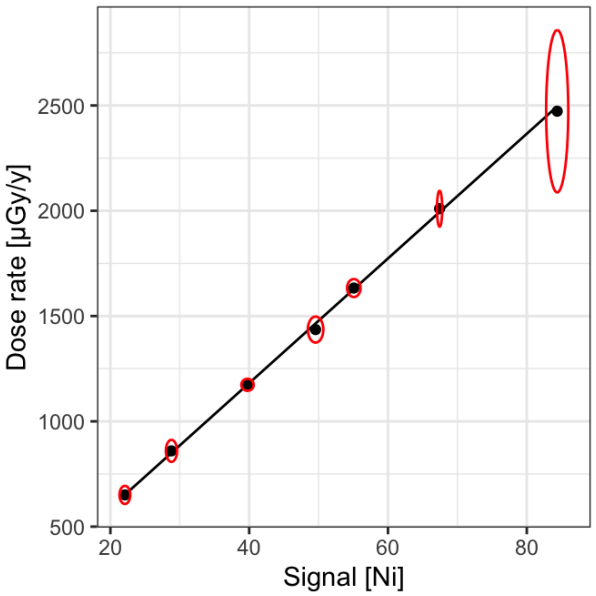

Figure 3. Built-in LaBr calibration curve in used at the CRP2A laboratory (Bordeaux).

4. Conclusions

The ‘gamma’ package is distributed over the Comprehensive **R** Archive Network (CRAN; http://cran.r-project.org). It is provided under the General Public Licence (GNU GPL3) conditions: the code is open and anyone can review it. Source code and installation instructions are available on GitHub at https://github.com/crp2a/gamma and https://github.com/crp2a/gammaShiny. Users are invited to contribute, share feedback, request new features or report bugs via the GitHub plateform. As for the ’Luminescence’ package (Kreutzer et al., 2012; Fuchs et al., 2015), future improvements to the ‘gamma’ package and associated GUI are intended to be community driven.

5. Acknowledgements

This work received a state financial support managed by the Agence Nationale de la Recherche (France) through the program *Investissements d’avenir* ref. 10-LABX-0052. The project leading to this publication has received funding from the Excellence Initiative of Aix-Marseille University - A*Midex, a French ’Investissements d’Avenir’ programme ref. 11-IDEX-0001. BL thanks Didier Miallier (Laboratoire de Physique de Clermont, UMR 6533) for his help during the calibration of the NaI probe.

References

Aitken, M. J. *An introduction to optical dating: the dating of quaternary sediments by the use of photon-stimulated luminescence*. Oxford University Press, 1998.

Casanovas, R., Morant, J., and Salvadó, M. *Temperature Peak-Shift Correction Methods for NaI(Tl) and $LaBr_3(Ce)$ Gamma-Ray Spectrum Stabilisation*. Radiation Measurements, 47(8): 588–595, 2012. doi: 10.1016/j.radmeas.2012.06.001.

Chang, W., Cheng, J., Allaire, J., Xie, Y., and McPherson, J. *shiny: Web Application Framework for R*, 2020. URL https://CRAN.R-project.org/package=shiny. R package version 1.5.0.

Fuchs, M. C., Kreutzer, S., Burow, C., Dietze, M., Fischer, M., Schmidt, C., and Fuchs, M. *Data Processing in Luminescence Dating Analysis: An Exemplary Workflow Using the R Package 'Luminescence'*. Quaternary International, 362: 8–13, 2015. doi: 10.1016/j.quaint.2014.06.034.

Gilmore, G. R. *Practical Gamma-Ray Spectrometry*. John Wiley & Sons, Ltd, 2^{nd} edition, 2008. ISBN 978-0-470-86198-1 and 978-0-470-86196-7.

Gorry, P. A. *General Least-Squares Smoothing and Differentiation by the Convolution (Savitzky-Golay) Method*. Analytical Chemistry, 62(6): 570–573, 1990. doi: 10.1021/ac00205a007.

Guérin, G. and Mercier, N. *Determining Gamma Dose Rates by Field Gamma Spectroscopy in Sedimentary Media: Results of Monte Carlo Simulations*. Radiation Measurements, 46(2): 190–195, 2011. doi: 10.1016/j.radmeas.2010.10.003.

Klusoň, J. *In-Situ Gamma Spectrometry in Environmental Monitoring*. Applied Radiation and Isotopes, 68(4): 529–535, 2010. doi: 10.1016/j.apradiso.2009.11.041.

Kreutzer, S., Schmidt, C., Fuchs, M. C., Dietze, M., Fischer, M., and Fuchs, M. *Introducing an R Package for Luminescence Dating Analysis*. Ancient TL, 30(1): 1–8, 2012.

Kreutzer, S., Burow, C., Dietze, M., Fuchs, M. C., Fischer, M., and Schmidt, C. *Software in the Context of Luminescence Dating: Status, Concepts and Suggestionsexemplified by the R Package 'Luminescence'*. Ancient TL, 35(2): 1–11, 2017.

Mercier, N. and Falguères, C. *Field Gamma Dose-Rate Measurement with a NaI(Tl) Detector: Re-Evaluation of the "Threshold" Technique*. Ancient TL, 25(1): 1–4, 2007.

Miallier, D., Guérin, G., Mercier, N., Pilleyre, T., and Sanzelle, S. *The Clermont Radiometric Reference Rocks: A Convenient Tool for Dosimetric Purposes*. Ancient TL, 27(2): 37–44, 2009.

Morháč, M. and Matoušek, V. *Peak Clipping Algorithms for Background Estimation in Spectroscopic Data*. Applied Spectroscopy, 62(1): 91–106, 2008. doi: 10.1366/000370208783412762.

Morháč, M., Kliman, J., Matoušek, V., Veselský, M., and Turzo, I. *Background Elimination Methods for Multidimensional Coincidence gamma-Ray Spectra*. Nuclear Instruments and Methods in Physics Research Section A: Accelerators, Spectrometers, Detectors and Associated Equipment, 401(1): 113–132, 1997. doi: 10.1016/S0168-9002(97)01023-1.

Murray, A. S., Bowman, S. G. E., and Aitken, M. J. *Evaluation of the Gamma Dose-Rate Contribution*. In Zimmerman, D. W., Aitken, M. J., and Mejdahl, V. (eds.), *A Specialist Seminar on Thermoluminescence Dating*, volume 2 of *PACT*, pp. 84–96. Conseil de l'Europe, 1978.

R Core Team. *R: A Language and Environment for Statistical Computing*. R Foundation for Statistical Computing, Vienna, Austria, 2020. URL https://www.R-project.org/.

Ryan, C., Clayton, E., Griffin, W., Sie, S., and Cousens, D. *SNIP, a Statistics-Sensitive Background Treatment for the Quantitative Analysis of Pixe Spectra in Geoscience Applications*. Nuclear Instruments and Methods in Physics Research Section B: Beam Interactions with Materials and Atoms, 34(3): 396–402, 1988. doi: 10.1016/0168-583X(88)90063-8.

Savitzky, A. and Golay, M. J. E. *Smoothing and Differentiation of Data by Simplified Least Squares Procedures.* Analytical Chemistry, 36(8): 1627–1639, 1964. doi: 10.1021/ac60214a047.

York, D., Evensen, N. M., Martínez, M. L., and De Basabe Delgado, J. *Unified Equations for the Slope, Intercept, and Standard Errors of the Best Straight Line*. American Journal of Physics, 72(3): 367–375, 2004. doi: 10.1119/1.1632486.

Reviewer

Martin Autzen

Thesis Abstracts

Index

Eslem Ben Arous

Chronology of human populations in North-western Africa during the Upper Pleistocene: chronological multi-methods approach (ESR/US, OSL and C-14) applied to Rabat-Témara sites

December 2019

Museum national d'Histoire naturelle –
UMR 7194 HNHP, Paris, France

Degree: Ph.D.

Supervisors: Christophe Falguères and Roland Nespoulet

During the last decades, research in Morocco has greatly highlighted the importance to consider North-western Africa in the study the dispersal of early *Homo sapiens* within and out of Africa over the Upper Pleistocene. For these issues, the Rabat-Témara region is a rare example for having preserved from the last 120,000 years human stratified occupations in six caves. These human occupations are attributed to the Middle Stone Age (MSA) and the Later Stone Age (LSA).

However, the current chronological framework in Témara is subject to many questions, both geochronological/methodological and cultural. In order to solve them, a new geochronological campaign was undertaken at El Harhoura 2 and El Mnasra. These two caves were recognized as essential for two main issues: (1) the early *Homo sapiens* coastal occupations linking the earliest examples of cognitive complexity evidence and exploitation of the marine resources during the MSA and (2) the cultural and populations shift traduced by the transition from the MSA to the LSA.

These caves have been the subject of optically stimulated luminescence (OSL) dating, published in 2012 and, preliminary combined US-ESR dating published in 2012. In this thesis, we re-investigated their chronological framework, using a multi-dating chronological approach based on the inter-comparisons of various results: OSL on quartz grain samples, combined US-ESR on teeth enamel and radiocarbon on seed and charcoal from archaeological hearths.

The inter-comparisons of the new 39 dates obtained in this work with previous dating work has shown the close correspondence between the radiocarbon and the US-ESR ages and has revealed: (1) a systematic discrepancy between all US-ESR ages and all OSL ages (OSL ages are systematically 25-50% older than US-ESR ages) and (2) discrepancy between OSL ages in different studies that can be as high as 40%. Reasons for these discrepancies are not yet fully understood and remain ambiguous because they can be explained with multiple causes (post-depositional mixing grains, the effect of variations in the beta dose rate to individual grains, incomplete bleaching,...).

At El Harhoura 2, these ages are enabled to date the end of the MSA around 40, 000 years ago, either 15,000 years younger than previous dates. For the first time, we propose LSA presence from 12,000 years to 8,000 years, covering Marine Isotopic Stage (MIS) 1. New dates allow us to identify a chronological hiatus of about 30,000 years between the end of the MSA and the LSA (formerly 45,000 years before this work). This absence of ages extends from the end of MIS 3 to MIS 2. As a result of this work, we built the first chronological model of the Rabat-Témara region at the North African scale, showing that new dating results have clear and direct implications to interpret human settlement dynamics: the absence of human populations from the end of the MIS 3 until the MIS 1 in this region is associated to a major environmental and climatic change.

At El Mnasra cave, the most intensive MSA human occupations which yielded evidence of marine shells exploitation (food and ornaments purposes) have been dated between 65,000 and 100,000 years, about 10,000 to 15,000 years younger than the OSL ages published in 2012. While previous single-grain ages of these levels associated them with periods of high sea levels, the new results bring more nuance. Indeed, the large analytical errors associated with the ages (this study and previous studies) shows that the chronological resolution of these occupations is not precise enough to validate this model.

A PDF of this thesis can be requested from the author at eslem.ben-arous@mnhn.fr or at ben-arous@shh.mpg.de

Lucas Sátiro do Carmo

Nuclear Radiation Importance on Archeological and Geological Dating – Application To Sediments Dating From Cabo Frio

April 2020

Institute for Nuclear and Energy Research , São Paulo, Brazil

Degree: Ph.D.

Supervisor: Shigueo Watanabe

In this work, a dunefield known as Dama Branca

(Brazil) has been dated using the following techniques: Optically Stimulated Luminescence (OSL), Thermoluminescence (TL) and Electronic Spin Resonance (ESR). Sediments have been collected from several points to study age distribution throughout Dama Branca. These ages are related to events of sediment transportation and stabilization. For Dama Branca specifically, variables related to weather such as rainfall and wind power are suspected to be responsible for its formation. OSL results were obtained applying the SAR protocol. TL and ESR results were obtained using the Multiple Aliquot Additive Dose protocol (MAAD). With respect to ESR measurements, the Ti-Li center was chosen for dating since it can be completely bleached by sun light exposure, which makes it suitable for aeolian sediment dating. The Ti-Li center is strongly dependent upon preheat, its stability has been assessed and a preheat temperature of 180 °C was selected. OSL ages are within 0.05 x 10^3 and 2.05 x 10^3 years. TL ages agree with OSL ages for samples collected from the dune base, however there are discrepancies between OSL and TL ages for the DBM2BASE sample, suggesting that it underwent a quicker burial process. ESR results are satisfactory for two samples, 2DB10 and 2DB11 (they follow OSL and TL results). The ages were compared to a simplified morphological study. In recent works about the weather in the Cabo Frio region it has been seen that the studied areas were formed under influence of arid conditions and cold water, variables that control sediment transportation in the region.

A PDF of this thesis can be downloaded from: https://doi.org/10.11606/T.85.2020.tde-17092020-152716

Ștefana-Mădălina Groza-Săcaciu

Revisiting optically stimulated luminescence chronologies on loess-paleosol master sections from Europe and beyond

November 2020

Faculty of Environmental Science and Engineering, Babeș-Bolyai University, Cluj-Napoca, Romania

Degree: Ph.D.

Supervisor: Alida Timar-Gabor

Optically stimulated luminescence (OSL) is linked to Quaternary research, especially in what regards loess-paleosol sections of paleoenvironmental and archeological importance. At Mircea Vodă, an interlaboratory exercise on a new set of samples confirmed previous discrepancies between quartz fractions as well as the age underestimations for older samples. The Pleistocene/Holocene samples yielded an earlier age discrepancy ($> \sim 20$ ka). Mircea Vodă was further investigated alongside Râmnicu Sărat for OSL and magnetic susceptibility analysis in order to assess the Pleistocene/Holocene transition. It was concluded that the time variation of the MS record across the transition is rather synchronous for these two sites and two other regional sites (Roxolany-Ukraine and Mošorin – Serbia), with the onset of increase of the magnetic susceptibility signal dated through OSL starting closer to the 17-ka transition from the benthic δ^{18}O record. High-resolution luminescence dating on the Pleistocene/Holocene transition was performed at Luochuan, China, to check for hiatuses due to erosional events. No hiatuses were observed but the OSL ages were highly variable and showed multiple inversions, most probably due to significant vertical mixing. At Krems-Wachtberg, a well-known archeological site from Austria, the average from CW-OSL and POSL ages for the horizons bracketing the archaeological layer is 32.4 $\pm$ 1.5 ka, thus agreeing within error limits with the previous chronological results. Establishing a robust chronology at the LGM site Kammern-Grubgraben managed to clarify certain aspects regarding the complex stratigraphy and geochronology.

Maryam Heydari

Applying Bayesian models to improve luminescence-based chronologies of Middle to Upper Palaeolithic sites in Iran

August 2020

Université Bordeaux Montaigne, Pessac, France

Degree: Ph.D.

Supervisors: Chantal Tribolo, Pierre Guibert, Guillaume Guérin

Statistical data analysis is a fundamental aspect of luminescence dating. For decades, data processing predominantly employed the frequentist (classic) school of thinking. Only recently, the development of Bayesian modelling specifically for luminescence dating in R environment, has provided an alternative. This thesis aims firstly to discuss the benefits of applying Bayesian models over the frequentist approach, and secondly to provide the first luminescence-based chronologies for Middle-Upper Palaeolithic key sites in Iran. Due to its location at the intersection between Africa, Europe and Central Asia, the Iranian plateau is of importance in tracking human dispersal over time. Despite this, there are very few chronologies spanning the Palaeolithic period in Iran. This thesis focuses on three key sites: Mirak, located at the margin of the central Iranian desert, the site of Ghār-e Boof in the southern Zagros Mountains, and Bawa Yawan in the central Zagros Mountains. Bayesian modelling of chronologies produced for the site of Mirak, date Upper, Intermediate and Middle Palaeolithic assemblages to 21 – 28 ka, 26 – 33 ka and 43 – 55 ka (95% CI) respectively. For the site of Ghār-e Boof, the Upper Palaeolithic culture was dated to 37 – 42 ka (95% CI) and the Middle Palaeolithic culture to 44 – 84 ka (95% CI). Elsewhere in Bawa Yawan, ages spanning 56 – 90 ka (95% CI) were obtained for assemblages attributed to the Middle Palaeolithic. The chronological study also revealed an age range of 12 – 16 ka for a unit attributed to the Epipalaeolithic culture.

Based on the study of these sites, this thesis explores the essential aspect of applying Bayesian methods in luminescence dating. The ideas which were particularly discussed were the benefits of Bayesian models to address systematic shared errors between samples and the ability to include independent chronological information, such as stratigraphic constraints or radiocarbon ages. This has helped to improve the precision of the Palaeolithic chronologies for Iran. Furthermore, this thesis tests the ability of Bayesian models to obtain an accurate central dose for well-bleached samples compared to one frequentist model, when quartz signals are close to saturation or when beta-dose rate heterogeneity in the surrounding sediment is high.

A PDF version of this thesis is available on request the author at mariheyd@gmail.com.

Maike Nowatzki

Aeolian Landforms as Palaeo Wind Indicators - Application of Geoinformatics and Optically Stimulated Luminescence Methods to Analyse Dunefields in the Ili-Balkhash Region (Kazakhstan)

June 2020

Department of Geography, University of Tübingen, Tübingen, Germany and Max Planck Institute for Chemistry, Mainz, Germany

Degree: M.Sc.

Supervisors: Hans-Joachim Rosner (Department of Geography, University of Tübingen), Kathryn Fitzsimmons (Max Planck Institute for Chemistry, Mainz)

Drylands currently cover almost half of the earth's land surface and are predicted to extend further due to human and climate change induced desertification. A significant part of the world's population will thus be affected by land degradation and other dryland hazards such as sand and dust storms or dune encroachments. The uncertainty of future developments render dryland research essential in order to provide scientific input for policy making. Palaeoclimatological studies in dryland settings as well as the examination of fundamental processes in dryland systems such as dunefields are therefore crucial. This study's research area, the Ili-Balkhash region, provides an optimal setting for such studies due to its richness in aeolian dryland forms. Additionally, Central Asia is predicted to be particularly challenged by the effects of climate change.

This thesis attempts to tackle the reconstruction of wind directions from dune orientations using remote sensing and GIS (Geographic Information Systems) methodology. A semi-automated algorithm for dune mapping and the quantification of dune orientations is presented and fully applied to two, partly applied to four dunefields in the Ili-Balkhash region. The algorithms are implemented using a combination of JavaScript and Python scripts run on the Google Earth Engine and pyQGIS, respectively. Dune mapping is conducted applying object-based image analysis (OBIA). Different types of primary data (optical satellite imagery and a digital elevation model) as well as secondary data derived thereof (filtered satellite imagery, dune height, slope data, and a vegetation index) are used to perform image segmentation and subsequent supervised classification. The calculation of dune orientations is exercised applying oriented bounding boxes around the dune features that have resulted from the image classification.

In order to connect dune orientations to (palaeo) wind behaviour, modern wind data is used to test for its compatibility with dune orientation patterns in three dunefields. Bedform trends are predicted from wind data based on the maximum gross bedform-normal transport rule (MGBNT). Additionally, Optically Stimulated Luminescence (OSL) analyses are conducted to date selected dunes and examine if OSL behaviour can be used to draw conclusions about sediment provenance.

The bedform trend prediction yields partial consensus with the observed dune orientations, suggesting that modern wind regimes might not exclusively be responsible for the present dune morphologies. Given the Middle Holocene ages that were established for two dunes, a difference between dune-forming wind regimes and the modern wind regime appears possible. However, further research taking into account other parameters influencing dune orientation (e.g. sediment supply) needs to be conducted to confirm this hypothesis.

A pdf of this thesis can be acquired by contacting the author (maike.nowatzki@ouce.ox.ac.uk)

Miriam Saleh

TL, OSL and IRSL dating on ancient ceramics in the context of the European project nEU-MED

October 2020

Dipartimento di Scienza dei Materiali, Università degli Studi di Milano-Bicocca, and Dipartimento di Fisica, Università degli Studi di Milano (Italy)

Degree: M.Sc.

Supervisors: Anna Galli, Letizia Bonizzoni

The aim of this thesis was to compare the data obtained with OSL and IRSL dating on ceramic materials with those achieved with the well-established thermoluminescence (TL) dating protocols. The work was carried out at LAMBDA Laboratory (LAboratory of Milano Bicocca University for Dating and Archaeometry) of Material Science Department of Milano-Bicocca University.

In detail, the main goal of nEU-MED European project is evaluating the economic development from the 7^{th} to the 9^{th} century between Northern Europe, and the territories of southern Europe still influenced by the late Roman domination. To understand difference among these situations nEU-MED's archaeologists spent on the study of ceramics artefacts. The area chosen for the analysis was the northern Maremma (Tuscany).

Twelve samples belonging to three different archaeological sites, were prepared with the "fine-grain" technique, 30 aliquots each one. TL dating was performed using a home-made system developed in LAMBDA Laboratory and based on the photon counting technique with a photomultiplier tube (EMI 9635QB) coupled to blue filters (Corning BG12). For OSL and IRSL measurement has been used the Risø TL / OSL system DA-20. Artificial irradiations were carried out by a 1400 MBq ^{90}Sr - ^{90}Y beta source and a 37 MBq ^{241}Am alpha source. For the dose rate evaluation, internal annual alpha and beta dose-rates were obtained by total alpha counting with ZnS scintillator discs and flame photometry analysis. For the measurement of paleodose with thermoluminescence, we applied the dose additive protocol (beta imparted dose: 3.51, 7.02 and 10.53 Gy). Moreover, OSL and IRSL measurements were carried out by applying the SAR protocol. The pre-heat value was experimentally derived based on the results of a dose recovery pre-heat plateau test.

By applying the recycling ratio, recuperation, and dose recovery tests, it was evident that not all samples showed the minimal criteria of acceptability. The main problem associated with OSL and IRSL dating was a low natural signal, especially in OSL measurements, perhaps due to low signal intensity emitted by quartz. As well as some TL measures are afflicted by low reproducibility of natural glow peak and saturation of signal.

Afterwards, we identified five samples datable by at least two of three dating techniques. The thermoluminescence results cover a large time span ($7^{th} - 11^{th}$ centuries): two samples are assumed to be 7^{th}-century potteries (618 $\pm$ 61 AD; 665 $\pm$ 66 AD), while three ceramics belong to the 10^{th}-century (999 $\pm$ 63 AD; 976 $\pm$ 95 AD; 1114 $\pm$ 100 AD). These two conclusions are in very good agreement with historical records and age hypothesized in advance by archaeologists, who assume in the analysed area a preponderant human presence between the 8^{th} and 11^{th} centuries. Furthermore, the IRSL results are to be considered good compared to poor results received from the OSL analysis. In fact, IRSL dating corresponds to the age given by the thermoluminescence, considered the error range. The potteries dated by TL at 7^{th} century, give the same results with IRSL dating (687 $\pm$ 16 AD; 574 $\pm$ 25 AD). One sample of the already mentioned group of three samples confirms the previous TL result (939 $\pm$ 29 AD), the last two datable samples appear to be younger on the IRSL analysis (1311 $\pm$ 65 AD, 1514 $\pm$ 74 AD). On the other hand, the OSL measures, in addition to being affected by high errors, do not coincide with the results of the TL and IRSL measures.

Although the obtained data are very preliminary, it was still possible to provide further information to complete the historical information concerning nEU-MED project aim. In addition, the good results of the IRSL analysis suggest that the ceramic body is dominated by feldspar minerals instead of the quartz. Moreover, we can consider this thesis a preliminary assessment of the comparison between the techniques used.

W.M. (Marijn) van der Meij

Co-evolution of soils and landscapes in the Anthropocene – from natural to intensively managed landscapes

November 2020

Department of Environmental Sciences, Wageningen University and Research, Wageningen, The Netherlands

Degree: Ph.D.

Supervisors: Jakob Wallinga, Michael Sommer, Arnaud J.A.M. Temme

The aim of my thesis is to identify and quantify how soils and landscape have evolved and possibly co-evolved during the transition from natural land cover to intensive land management in the Anthropocene.

As study site I use the landscape laboratory CarboZALF D. CarboZALF D is a kettle-hole catchment of 4 ha with elevation differences up to 8 meters, located in north-eastern Germany. The colluvium in the closed kettle hole catchment provides a complete geo-archive of landscape change. We reconstruct the paleosurface of study site Carbo-ZALF-D prior to the anthropogenic erosion. We used an extensive dataset of soil descriptions, which enabled a detailed spatial estimate of erosion and deposition by estimating erosion based on soil profile truncations and deposition based on colluvium thickness. We reconstruct the rates of deposition in Carbo-ZALF-D using Optically Stimulated Luminescence (OSL) dating. The reworking of colluvial sediments by tillage causes two challenges for OSL dating: grains with different depositional ages become mixed and grains become exposed to daylight even long after they are deposited. We present a novel methodology where we combine OSL dating with advanced age modelling and an archaeological reconstruction of historical land use to correct for this post-depositional bleaching. Our results show a 100-fold increase in deposition rates, starting around 5000 years ago. The kettle hole shows a complex spatiotemporal pattern of colluvial infilling and landscape evolution, which we were only able to reconstruct using a high OSL sampling density and extensive soil geomorphic research.

To simulate the evolution of soils and landscapes under varying climatic and anthropogenic forcing, we review the role of water as dominant driver in natural soil and landscape evolution and its potential as driver in simulations with soil-landscape evolution models (SLEMs). The co-evolution of soils, topography and the hydrological system is essential for understanding the response of soils and landscapes to changes in climate. However, this co-evolution can currently not be simulated over long timescales with SLEMs due to several conceptual and methodological challenges. We provide partial solutions for these challenges to develop our SLEM HydroLorica. HydroLorica simulates soil and landscape evolution with various dynamic drivers such as water flow, vegetation type and land use. We included additional essential processes such as tree throw, soil creep and tillage. We use HydroLorica to simulate the evolution of soils

and landscape under various rainfall and land-use scenarios for an artificial undulating landscape. The results show that cultivation of natural landscapes increases soil heterogeneity, but also increases correlations between soil and terrain properties. Our results confirm that humans have become the dominant soil forming factor in intensively managed landscapes.

The development of HydroLorica, with water flow as explicit driver and with increased process coverage, is a big step forward in soil-landscape evolution modelling. A combination of reconstruction and simulation methods is essential for developing and testing hypotheses of soil-landscape co-evolution. Soil-landscape evolution in natural and intensively managed landscapes have different characteristics due to different driving forces and dominant processes. In intensively managed landscapes, disturbance rates are much higher than in natural settings. As a consequence, slowly developing soil properties degrade, while fast-developing soil properties can form a new equilibrium. As a consequence, co-evolution does not occur in the sense that it does in natural settings, because interactions between landscape components are missing. However, the management of soils and landscapes is often adapted to counteract unintended changes to soils and landscapes under earlier management. In intensively managed landscapes, land management may thus co-evolve with the rest of the landscape.

A PDF of this thesis can be downloaded from: https://www.researchgate.net/publication/341670234

Bibliography

Compiled by Sebastien Huot

From 1st June 2020 to 31st November 2020

Special issue

- Electron spin resonance (ESR) dating in Quaternary studies: evolution, recent advances and applications, Mathieu Duval, Gilles Rixhon, Lee J. Arnold ed. Quaternary International

Azevedo, R.L., Asfora, V.K., Mützenberg, D.S., Cisneiros, D., Sullasi, H.L., Kinoshita, A.M., Guzzo, P.L., Skinner, A.R., Baffa, O., Pessis, A.-M., Khoury, H.J., 2020. ESR dating of megafauna enamel teeth from Lagoa Uri de Cima Archaeological Site (Pernambuco, Northeastern Brazil). Quaternary International 556, 38-48. http://doi.org/10.1016/j.quaint.2019.02.039

Bahain, J.-J., Duval, M., Voinchet, P., Tissoux, H., Falguères, C., Grün, R., Moreno, D., Shao, Q., Tombret, O., Jamet, G., Faivre, J.-P., Cliquet, D., 2020. ESR and ESR/U-series chronology of the Middle Pleistocene site of Tourville-la-Rivière (Normandy, France) - A multi-laboratory approach. Quaternary International 556, 58-70. http://doi.org/10.1016/j.quaint.2019.06.015

Bartz, M., Duval, M., Brill, D., Zander, A., King, G.E., Rhein, A., Walk, J., Stauch, G., Lehmkuhl, F., Brückner, H., 2020. Testing the potential of K-feldspar pIR-IRSL and quartz ESR for dating coastal alluvial fan complexes in arid environments. Quaternary International 556, 124-143. http://doi.org/10.1016/j.quaint.2020.03.037

Beerten, K., Verbeeck, K., Laloy, E., Vanacker, V., Vandenberghe, D., Christl, M., De Grave, J., Wouters, L., 2020. Electron spin resonance (ESR), optically stimulated luminescence (OSL) and terrestrial cosmogenic radionuclide (TCN) dating of quartz from a Plio-Pleistocene sandy formation in the Campine area, NE Belgium. Quaternary International 556, 144-158. http://doi.org/10.1016/j.quaint.2020.06.011

Ben Arous, E., Falguères, C., Tombret, O., El Hajraoui, M.A., Nespoulet, R., 2020. Combined US-ESR dating of fossil teeth from El Harhoura 2 cave (Morocco): New data about the end of the MSA in Temara region. Quaternary International 556, 88-95. http://doi.org/10.1016/j.quaint.2019.02.029

Demuro, M., Arnold, L.J., Duval, M., Méndez-Quintas, E., Santonja, M., Pérez-González, A., 2020a. Refining the chronology of Acheulean deposits at Porto Maior in the River Miño basin (Galicia, Spain) using a comparative luminescence and ESR dating approach. Quaternary International 556, 96-112. http://doi.org/10.1016/j.quaint.2020.01.005

Demuro, M., Duval, M., Arnold, L.J., Spooner, N.A., Creighton, D.F., Méndez-Quintas, E., Santonja, M., Pérez-González, A., 2020b. Insights into the relationship between luminescence and ESR dating signals from Spanish sedimentary quartz samples of different geologic origins. Quaternary International 556, 165-179. http://doi.org/10.1016/j.quaint.2020.05.037

Duval, M., Arnold, L.J., Rixhon, G., 2020a. Electron spin resonance (ESR) dating in Quaternary studies: evolution, recent advances and applications. Quaternary International 556, 1-10. http://doi.org/10.1016/j.quaint.2020.07.044

Duval, M., Voinchet, P., Arnold, L.J., Parés, J.M., Minnella, W., Guilarte, V., Demuro, M., Falguères, C., Bahain, J.-J., Despriée, J., 2020b. A multi-technique dating study of two Lower Palaeolithic sites from the Cher Valley (Middle Loire Catchment, France): Lunery-la Terre-des-Sablons and Brinay-la Noira. Quaternary International 556, 71-87. http://doi.org/10.1016/j.quaint.2020.05.033

Falguères, C., 2020. A French story of the ESR dating method for Quaternary samples. Quaternary International 556, 11-19. http://doi.org/10.1016/j.quaint.2019.09.047

Grün, R., 2020. A very personal, 35 years long journey in ESR dating. Quaternary International 556, 20-37. http://doi.org/10.1016/j.quaint.2018.11.038

Molodkov, A., 2020. The Late Pleistocene palaeoenvironmental evolution in Northern Eurasia through the prism of the mollusc shell-based ESR dating evidence. Quaternary International 556, 180-197. http://doi.org/10.1016/j.quaint.2019.05.031

Richard, M., Falguères, C., Pons-Branchu, E., Richter, D., Beutelspacher, T., Conard, N.J., Kind, C.J., 2020. The Middle to Upper Palaeolithic transition in Hohlenstein-Stadel cave (Swabian Jura, Germany): A comparison between ESR, U-series and radiocarbon dating. Quaternary International 556, 49-57. http://doi.org/10.1016/j.quaint.2019.04.009

Richter, M., Tsukamoto, S., Long, H., 2020. ESR dating of Chinese loess using the quartz Ti centre: A comparison with independent age control. Quaternary International 556, 159-164. http://doi.org/10.1016/j.quaint.2019.04.003

Schellmann, G., Schielein, P., Burow, C., Radtke, U., 2020. Accuracy of ESR dating of small gastropods from loess and fluvial deposits in the Bavarian Alpine Foreland. Quaternary International 556, 198-215. http://doi.org/10.1016/j.quaint.2019.07.026

Schielein, P., Burow, C., Pajon, J., Rojas Consuegra, R., Zhao, J.-x., Schellmann, G., 2020. ESR and U-Th dating results for Last Interglacial coral reef terraces at the northern coast of Cuba. Quaternary International 556, 216-229. http://doi.org/10.1016/j.quaint.2019.11.041

Voinchet, P., Pereira, A., Nomade, S., Falguères, C., Biddittu, I., Piperno, M., Moncel, M.H., Bahain, J.J., 2020. ESR dating applied to optically bleached quartz - A comparison with 40Ar/39Ar chronologies on Italian Middle Pleistocene sequences. Quaternary International 556, 113-123. http://doi.org/10.1016/j.quaint.2020.03.012

Various geological applications

- aeolian

Bertran, P., Andrieux, E., Bateman, M.D., Fuchs, M., Klinge, M., Marembert, F., 2020. Mapping and chronology of coversands and dunes from the Aquitaine basin, southwest France. Aeolian Research 47, 100628. http://doi.org/10.1016/j.aeolia.2020.100628

Fitzsimmons, K.E., Nowatzki, M., Dave, A.K., Harder, H., 2020. Corrigendum to "Intersections between wind regimes, topography and sediment supply: Perspectives from aeolian landforms in Central Asia". Palaeogeography, Palaeoclimatology, Palaeoecology 540 (2020) 109531. Palaeogeography, Palaeoclimatology, Palaeoecology 552, 109795. http://doi.org/10.1016/j.palaeo.2020.109795

Follett, R.F., Stewart, C.E., Bradford, J., Pruessner, E.G., Sims, P.L., Vigil, M.F., 2020. Long-term pasture management impacts on eolian sand soils in the southern mixed-grass prairie. Quaternary International 565, 84-93. http://doi.org/10.1016/j.quaint.2020.07.019

Ji, J., Wang, G., Yang, L., Li, J., Xu, Y., Liu, Z., 2020. Holocene climate in arid central Asia and timing of sand dunes accumulation in Balikun Basin, Northwest China. Geological Journal 55, 7346-7358. http://doi.org/10.1002/gj.3655

Kaiser, K., Schneider, T., Küster, M., Dietze, E., Fülling, A., Heinrich, S., Kappler, C., Nelle, O., Schult, M., Theuerkauf, M., Vogel, S., de Boer, A.M., Börner, A., Preusser, F., Schwabe, M., Ulrich, J., Wirner, M., Bens, O., 2020. Palaeosols and their cover sediments of a glacial landscape in northern central Europe: Spatial distribution, pedostratigraphy and evidence on landscape evolution. CATENA 193, 104647. http://doi.org/10.1016/j.catena.2020.104647

Sizov, O., Konstantinov, A., Volvakh, A., Molodkov, A., 2020. Timing and Sedimentary Record of Late Quaternary Fluvio-Aeolian Successions of the Tura-Pyshma Interfluve (SW Western Siberia, Russia). Geosciences 10, 396. http://doi.org/10.3390/geosciences10100396

Xue, W., Jin, H., Liu, B., Sun, L., Liu, Z., 2020. History of moisture change indicated by aeolian deposit in the Horqin sandy land, Northeastern China since the Last Glacial Maximum. Quaternary International 547, 50-62. http://doi.org/10.1016/j.quaint.2019.12.022

- cave

Ballesteros, D., Álvarez-Vena, A., Monod-Del Dago, M., Rodríguez-Rodríguez, L., Sanjurjo-Sánchez, J., Álvarez-Lao, D., Pérez-Mejías, C., Valenzuela, P., DeFelipe, I., Laplana, C., Cheng, H., Jiménez-Sánchez, M., 2020. Paleoenvironmental evolution of Picos de Europa (Spain) during marine isotopic stages 5c to 3 combining glacial reconstruction, cave sedimentology and paleontological findings. Quaternary Science Reviews 248, 106581. http://doi.org/10.1016/j.quascirev.2020.106581

De Waele, J., Picotti, V., Martina, M.L.V., Brook, G., Yang, L., Forti, P., 2020. Holocene evolution of halite caves in the Cordillera de la Sal (Central Atacama, Chile) in different climate conditions. Geomorphology 370, 107398. http://doi.org/10.1016/j.geomorph.2020.107398

Utida, G., Cruz, F.W., Santos, R.V., Sawakuchi, A.O., Wang, H., Pessenda, L.C.R., Novello, V.F., Vuille, M., Strauss, A.M., Borella, A.C., Stríkis, N.M., Guedes, C.C.F., Dias De Andrade, F.R., Zhang, H., Cheng, H., Edwards, R.L., 2020. Climate changes in Northeastern Brazil from deglacial to Meghalayan periods and related environmental impacts. Quaternary Science Reviews 250, 106655. http://doi.org/10.1016/j.quascirev.2020.106655

- coastal

Bartz, M., Duval, M., Brill, D., Zander, A., King, G.E., Rhein, A., Walk, J., Stauch, G., Lehmkuhl, F., Brückner, H., 2020. Testing the potential of K-feldspar pIR-IRSL and quartz ESR for dating coastal alluvial fan complexes in arid environments. Quaternary International 556, 124-143. http://doi.org/10.1016/j.quaint.2020.03.037

Bateman, M.D., McHale, K., Bayntun, H.J., Williams, N., 2020. Understanding historical coastal spit evolution: A case study from Spurn, East Yorkshire, UK. Earth Surface Processes and Landforms 45, 3670-3686. http://doi.org/10.1002/esp.4991

Betancurth, L., Preusser, F., Mueller, D., Rambeau, C., Cañón, J., 2020. First luminescence chronology of late Holocene deposits of the tropical Atrato Delta, Colombia. Journal of South American Earth Sciences 104, 102813. http://doi.org/10.1016/j.jsames.2020.102813

Castillo, M., Muñoz-Salinas, E., Sanderson, D.C.W., Cresswell, A., 2020. Landscape evolution of Punta Arena sand spit (SE Baja California Peninsula, NW Mexico): Implications of ENSO on landscape erosion rates. CATENA 193, 104601. http://doi.org/10.1016/j.catena.2020.104601

Gao, L., Long, H., Tamura, T., Ye, L., Hou, Y., Shen, J., 2020. Refined chronostratigraphy of a late Quaternary Sedimentary sequence from the Yangtze River delta based on K-feldspar luminescence dating. Marine Geology 427, 106271. http://doi.org/10.1016/j.margeo.2020.106271

Gouramanis, C., Switzer, A.D., Bristow, C.S., Pham, D.T., Mauz, B., Hoang, Q.D., Lam, D.D., Lee, Y.S., Soria, J.L.A., Pile, J., Chi, N.T.K., Nghiem, D., Sloss, C., 2020. Holocene evolution of the Chan May coastal embayment, central Vietnam: Changing coastal dynamics associated with decreasing rates of progradation possibly forced by mid- to late-Holocene sea-level changes. Geomorphology 367, 107273. http://doi.org/10.1016/j.geomorph.2020.107273

Kennedy, D.M., Oliver, T.S.N., Tamura, T., Murray-Wallace, C.V., Thom, B.G., Rosengren, N.J., Ierodiaconou, D., Augustinus, P., Leach, C., Gao, J., McSweeney, S.L., Konlechner, T., Woodroffe, C.D., 2020. Holocene evolution of the Ninety Mile Beach sand barrier, Victoria, Australia: The role of sea level, sediment supply and climate. Marine Geology 430, 106366. http://doi.org/10.1016/j.margeo.2020.106366

Marra, F., Bahain, J.-J., Jicha, B.R., Nomade, S., Palladino, D.M., Pereira, A., Tolomei, C., Voinchet, P., Anzidei, M., Aureli, D., Ceruleo, P., Falguères, C., Florindo, F., Gatta, M., Ghaleb, B., La Rosa, M., Peretto, C., Petronio, C., Rocca, R., Rolfo, M.F., Salari, L., Smedile, A., Tombret, O., 2019. Reconstruction of the MIS 5.5, 5.3 and 5.1 coastal terraces in Latium (central Italy): A re-evaluation of the sea-level history in the Mediterranean Sea during the last interglacial. Quaternary International 525, 54-77. http://doi.org/10.1016/j.quaint.2019.09.001

Molodkov, A., 2020. The Late Pleistocene palaeoenvironmental evolution in Northern Eurasia through the prism of the mollusc shell-based ESR dating evidence. Quaternary International 556, 180-197. http://doi.org/10.1016/j.quaint.2019.05.031

Nalin, R., Lamothe, M., Auclair, M., Massari, F., 2020. Chronology of the marine terraces of the Crotone Peninsula (Calabria, southern Italy) by means of infrared-stimulated luminescence (IRSL). Marine and Petroleum Geology 122, 104645. http://doi.org/10.1016/j.marpetgeo.2020.104645

Normand, R., Simpson, G., Herman, F., Biswas, R.H., Bahroudi, A., 2019. Holocene sedimentary record and coastal evolution in the Makran Subduction Zone (Iran). Quaternary 2, 21. http://doi.org/10.3390/quat2020021

Oliver, T.S.N., Tamura, T., Brooke, B.P., Short, A.D., Kinsela, M.A., Woodroffe, C.D., Thom, B.G., 2020. Holocene evolution of the wave-dominated embayed Moruya coastline, southeastern Australia: Sediment sources, transport rates and alongshore interconnectivity. Quaternary Science Reviews 247, 106566. http://doi.org/10.1016/j.quascirev.2020.106566

Parker, A.G., Morley, M.W., Armitage, S.J., Engel, M., Parton, A., Preston, G.W., Russ, H., Drechsler, P., 2020. Palaeoenvironmental and sea level changes during the Holocene in eastern Saudi Arabia and their implications for Neolithic populations. Quaternary Science Reviews 249, 106618. http://doi.org/10.1016/j.quascirev.2020.106618

Rodrigues, F.C.G., Giannini, P.C.F., Fornari, M., Sawakuchi, A.O., 2020. Deglacial climate and relative sea level changes forced the shift from eolian sandsheets to dunefields in southern Brazilian coast. Geomorphology 365, 107252. http://doi.org/10.1016/j.geomorph.2020.107252

Rosentau, A., Nirgi, T., Muru, M., Bjursäter, S., Hang, T., Preusser, F., Risberg, J., Sohar, K., Tõnisson, H., Kriiska, A., 2020. Holocene relative shore level changes and Stone Age hunter-gatherers in Hiiumaa Island, eastern Baltic Sea. Boreas 49, 783-798. http://doi.org/10.1111/bor.12452

Sanderson, D.C.W., Kinnaird, T.C., 2019. Optically stimulated luminescence dating as a geochronological tool for Late Quaternary sediments in the Red Sea region, in: Rasul, N.M.A., Stewart, I.C.F. (Eds.), Geological Setting, Palaeoenvironment and Archaeology of the Red Sea. Springer International Publishing, Cham, pp. 685-707. http://doi.org/10.1007/978-3-319-99408-6_31

Schielein, P., Burow, C., Pajon, J., Rojas Consuegra, R., Zhao, J.-x., Schellmann, G., 2020. ESR and U-Th dating results for Last Interglacial coral reef terraces at the northern coast of Cuba. Quaternary International 556, 216-229. http://doi.org/10.1016/j.quaint.2019.11.041

Tamura, T., Ta, T.K.O., Saito, Y., Bateman, M.D., Murray-Wallace, C.V., Nguyen, T.M.L., Sato, T., Nguyen, V.L., 2020. Seasonal control on coastal dune morphostratigraphy under a monsoon climate, Mui Ne dunefield, SE Vietnam. Geomorphology 370, 107371. http://doi.org/10.1016/j.geomorph.2020.107371

Zurbuchen, J., Simms, A.R., Huot, S., 2020. Episodic coastal progradation of the Oxnard Plain, Southern California, USA. Journal of Coastal Research 36, 1130-1144. http://doi.org/10.2112/JCOASTRES-D-19-00125.1

- colluvial

Colarossi, D., Duller, G.A.T., Roberts, H.M., Tooth, S., Botha, G.A., 2020. A comparison of multiple luminescence chronometers at Voordrag, South Africa. Quaternary Geochronology 60, 101094. http://doi.org/10.1016/j.quageo.2020.101094

Fonsêca, D.N., de Barros Corrêa, A.C., de Azevêdo Cavalcanti Tavares, B., Rodrigues de Lira, D., Magalhães de Barros, A.C., da Silva Mützenberg, D., 2020. Coupling of tectonic factors and precipitation variability as a driver of Late Quaternary aggradation in Northeast Brazil. Earth Surface Processes and Landforms 45, 3525-3539. http://doi.org/10.1002/esp.4982

Kaiser, K., Schneider, T., Küster, M., Dietze, E., Fülling, A., Heinrich, S., Kappler, C., Nelle, O., Schult, M., Theuerkauf, M., Vogel, S., de Boer, A.M., Börner, A., Preusser, F., Schwabe, M., Ulrich, J., Wirner, M., Bens, O., 2020. Palaeosols and their cover sediments of a glacial landscape in northern central Europe: Spatial distribution, pedostratigraphy and evidence on landscape evolution. CATENA 193, 104647. http://doi.org/10.1016/j.catena.2020.104647

- earthquake (and fault related)

Beerten, K., Verbeeck, K., Laloy, E., Vanacker, V., Vandenberghe, D., Christl, M., De Grave, J., Wouters, L., 2020. Electron spin resonance (ESR), optically stimulated luminescence (OSL) and terrestrial cosmogenic radionuclide (TCN) dating of quartz from a Plio-Pleistocene sandy formation in the Campine area, NE Belgium. Quaternary International 556, 144-158. http://doi.org/10.1016/j.quaint.2020.06.011

Cheon, Y., Choi, J.-H., Kim, N., Lee, H., Choi, I., Bae, H., Rockwell, T.K., Lee, S.R., Ryoo, C.-R., Choi, H., Lee, T.-H., 2020. Late Quaternary transpressional earthquakes on a long-lived intraplate fault: A case study of the Southern Yangsan Fault, SE Korea. Quaternary International 553, 132-143. http://doi.org/10.1016/j.quaint.2020.07.025

Divyadarshini, A., Singh, V., Jaiswal, M.K., Rawat, M., 2020. Exploring the roles of climate and tectonics in the geomorphic evolution of the Chitwan Intermontane valley, Central Himalaya. Geomorphology 367, 107298. http://doi.org/10.1016/j.geomorph.2020.107298

Oohashi, K., Minomo, Y., Akasegawa, K., Hasebe, N., Miura, K., 2020. Optically stimulated luminescence signal resetting of quartz gouge during subseismic to seismic frictional sliding: A case study using granite-derived quartz. Journal of Geophysical Research: Solid Earth 125, e2020JB019900. http://doi.org/10.1029/2020JB019900

Tokarski, A.K., Świerczewska, A., Lasocki, S., Cuong, N.Q., Strzelecki, P.J., Olszak, J., Kukulak, J., Alexanderson, H., Zasadni, J., Krąpiec, M., Mikołajczak, M., 2020. Active faulting and seismic hazard in the Outer Western Carpathians (Polish Galicia): Evidence from fractured Quaternary gravels. Journal of Structural Geology 141, 104210. http://doi.org/10.1016/j.jsg.2020.104210

Torabi, M., Fattahi, M., Amini, H., Ghassemi, M.R., Karimi, N., 2020. OSL dating of landslide-dammed-lake deposits in the North of Tehran, Iran: 958 Ray-Taleghan/Ruyan earthquake. Quaternary International 562, 46-57. http://doi.org/10.1016/j.quaint.2020.07.006

Trexler, C.C., Cowgill, E., Spencer, J.Q.G., Godoladze, T., 2020. Rate of active shortening across the southern thrust front of the Greater Caucasus in western Georgia from kinematic modeling of folded river terraces above a listric thrust. Earth and Planetary Science Letters 544, 116362. http://doi.org/10.1016/j.epsl.2020.116362

Tsakalos, E., Lin, A., Kazantzaki, M., Bassiakos, Y., Nishiwaki, T., Filippaki, E., 2020. Absolute dating of past seismic events using the OSL technique on fault gouge material—a case study of the Nojima Fault Zone, SW Japan. Journal of Geophysical Research: Solid Earth 125, e2019JB019257. http://doi.org/10.1029/2019JB019257

- fluvial

Agatova, A.R., Nepop, R.K., Bronnikova, M.A., Zhdanova, A.N., Moska, P., Zazovskaya, E.P., Khazina, I.V., 2020. Problems of 14C dating in fossil soils within tectonically active highlands of Russian Altai in the chronological context of the late Pleistocene megafloods. CATENA 195, 104764. http://doi.org/10.1016/j.catena.2020.104764

Bahain, J.-J., Duval, M., Voinchet, P., Tissoux, H., Falguères, C., Grün, R., Moreno, D., Shao, Q., Tombret, O., Jamet, G., Faivre, J.-P., Cliquet, D., 2020. ESR and ESR/U-series chronology of the Middle Pleistocene site of Tourville-la-Rivière (Normandy, France) - A multi-laboratory approach. Quaternary International 556, 58-70. http://doi.org/10.1016/j.quaint.2019.06.015

Benito-Calvo, A., Arnold, L.J., Mora, R., Martínez-Moreno, J., Demuro, M., 2020. Reconstructing Mousterian landscapes in the southeastern Pyrenees (Roca dels Bous site, Pre-Pyrenees ranges, Spain). Quaternary Research 97, 167-186. http://doi.org/10.1017/qua.2020.29

Blinkhorn, J., Achyuthan, H., Jaiswal, M., Singh, A.K., 2020. The first dated evidence for Middle-Late Pleistocene fluvial activity in the central Thar Desert. Quaternary Science Reviews 250, 106656. http://doi.org/10.1016/j.quascirev.2020.106656

Bonnet, S., Reimann, T., Wallinga, J., Lague, D., Davy, P., Lacoste, A., 2019. Landscape dynamics revealed by luminescence signals of feldspars from fluvial terraces. Scientific Reports 9, 8569. http://doi.org/10.1038/s41598-019-44533-4

Borgohain, B., Mathew, G., Chauhan, N., Jain, V., Singhvi, A.K., 2020. Evidence of episodically accelerated denudation on the Tibetan Namche Barwa massif by megafloods. Quaternary Science Reviews 245, 106410. http://doi.org/10.1016/j.quascirev.2020.106410

Dash, C., Jaiswal, M.K., Pati, P., Patel, N.K., Singh, A.K., Shah, R.A., 2020. Fluvial response to Late Quaternary sea level changes along the Mahanadi delta, east coast of India. Quaternary International 553, 60-72. http://doi.org/10.1016/j.quaint.2020.07.033

Gao, L., Wang, X., Yi, S., Vandenberghe, J., Gibling, M.R., Lu, H., 2018. Episodic sedimentary evolution of an alluvial fan (Huangshui catchment, NE Tibetan Plateau). Quaternary 1, 16. http://doi.org/10.3390/quat1020016

Kapannusch, R., Scherler, D., King, G., Wittmann, H., 2020. Glacial influence on late Pleistocene 10Be-derived paleo-erosion rates in the north-western Himalaya, India. Earth and Planetary Science Letters 547, 116441. http://doi.org/10.1016/j.epsl.2020.116441

Larkin, Z.T., Ralph, T.J., Tooth, S., Duller, G.A.T., 2020. A shifting 'river of sand': The profound response of Australia's Warrego River to Holocene hydroclimatic change. Geomorphology 370, 107385. http://doi.org/10.1016/j.geomorph.2020.107385

Mitrinović, D., Zarić, J., Anđelković, O., Sipos, G., Polomčić, D., Dimkić, M., 2020. Dating of alluvial sediments from borehole at the lower course of the Sava river and indications of the connection between their genesis and climate changes in the Pleistocene. Quaternary International 547, 75-85. http://doi.org/10.1016/j.quaint.2019.09.028

Olszak, J., Alexanderson, H., 2020. Post-IR IRSL dating the oldest (?) river terrace sediments in the Polish Outer Carpathians: Insights into the landscape evolution. Geomorphology 371, 107436. http://doi.org/10.1016/j.geomorph.2020.107436

Panda, S., Kumar, A., Das, S., Devrani, R., Rai, S., Prakash, K., Srivastava, P., 2020. Chronology and sediment provenance of extreme floods of Siang River (Tsangpo-Brahmaputra River valley), northeast Himalaya. Earth Surface Processes and Landforms 45, 2495-2511. http://doi.org/10.1002/esp.4893

Quik, C., Candel, J.H.J., Makaske, B., van Beek, R., Paulissen, M., Maas, G.J., Verplak, M., Spek, T., Wallinga, J., 2020. Anthropogenic drivers for exceptionally large meander formation during the Late Holocene. Anthropocene 32, 100263. http://doi.org/10.1016/j.ancene.2020.100263

Saynor, M., Wasson, R., Erskine, W., Lam, D., 2020. Holocene palaeohydrology of the East Alligator River, for application to mine site rehabilitation, Northern Australia. Quaternary Science Reviews 249, 106552. http://doi.org/10.1016/j.quascirev.2020.106552

Schellmann, G., Schielein, P., Burow, C., Radtke, U., 2020. Accuracy of ESR dating of small gastropods from loess and fluvial deposits in the Bavarian Alpine Foreland. Quaternary International 556, 198-215. http://doi.org/10.1016/j.quaint.2019.07.026

Sizov, O., Konstantinov, A., Volvakh, A., Molodkov, A., 2020. Timing and Sedimentary Record of Late Quaternary Fluvio-Aeolian Successions of the Tura-Pyshma Interfluve (SW Western Siberia, Russia). Geosciences 10, 396. http://doi.org/10.3390/geosciences10100396

Stange, K.M., Midtkandal, I., Nystuen, J.P., Murray, A., Sohbati, R., Thompson, W., Spiegel, C., Kuss, H.-J., 2019. Erosive response of non-glaciated Pyrenean headwater catchments to the last major climate transition and establishing interglacial conditions. Quaternary 2, 17. http://doi.org/10.3390/quat2020017

Vayssière, A., Castanet, C., Gautier, E., Virmoux, C., Dépret, T., Gandouin, E., Develle, A.-L., Mokadem, F., Saulnier-Copard, S., Sabatier, P., Carcaud, N., 2020. Readjustments of a sinuous river during the last 6000 years in northwestern Europe (Cher River, France): from an active meandering river to a stable river course under human forcing. Geomorphology 370, 107395. http://doi.org/10.1016/j.geomorph.2020.107395

Veldkamp, A., Schoorl, J.M., Claessens, L., Temme, A.J.A.M., Broers, A.G.M., van Orsouw, T.L., Voesten, M.T.C.M., Reimann, T., 2020. Preservation of the last aggradation phase in climate-driven terraces: Evidence from Late Quaternary reach-specific fluvial dynamics of the Allier River (France). Earth Surface Processes and Landforms 45, 3381-3395. http://doi.org/10.1002/esp.4972

Viveen, W., Baby, P., Sanjurjo-Sanchez, J., Hurtado-Enríquez, C., 2020. Fluvial terraces as quantitative markers of late Quaternary detachment folding and creeping thrust faulting in the Peruvian Huallaga basin. Geomorphology 367, 107315. http://doi.org/10.1016/j.geomorph.2020.107315

Voinchet, P., Pereira, A., Nomade, S., Falguères, C., Biddittu, I., Piperno, M., Moncel, M.H., Bahain, J.J., 2020. ESR dating applied to optically bleached quartz - A comparison with 40Ar/39Ar chronologies on Italian Middle Pleistocene sequences. Quaternary International 556, 113-123. http://doi.org/10.1016/j.quaint.2020.03.012

Wang, H., Tong, K., Hu, G., Wang, P., Li, D., Huang, J., Cao, G., Zhang, J., Chen, J., 2021. Dam and megafloods at the First Bend of the Yangtze River since the Last Glacial Maximum. Geomorphology 373, 107491. http://doi.org/10.1016/j.geomorph.2020.107491

Wu, C., Li, J., Zuza, A.V., Liu, C., Liu, W., Chen, X., Jiang, T., Li, B., 2020. Cenozoic cooling history and fluvial terrace development of the western domain of the Eastern Kunlun Range, northern Tibet. Palaeogeography, Palaeoclimatology, Palaeoecology 560, 109971. http://doi.org/10.1016/j.palaeo.2020.109971

Zhang, D., Wang, G., Pullen, A., Abell, J.T., Ji, J., Shen, T., 2020. Landscape evolution and development of eolian-modified unconsolidated gravel surfaces and yardangs in the Hami Basin, China. Geomorphology 368, 107355. http://doi.org/10.1016/j.geomorph.2020.107355

- glacial and periglacial

Gao, C., Huot, S., McDonald, A.M., Crabtree, D.C., Turton, C.L., 2020. Subtill nonglacial deposits and their climatic implications for the Last Interglacial (MIS 5e), Hudson Bay Lowlands, Canada. Quaternary Science Reviews 248, 106590. http://doi.org/10.1016/j.quascirev.2020.106590

Hu, G., Yi, C.-L., Liu, J.-H., Wang, P., Zhang, J.-F., Li, S.-H., Li, D., Huang, J., Wang, H.-y., Zhang, A.-m., Shi, L., Shui, X., 2020. Glacial advances and stability of the moraine dam on Mount Namcha Barwa since the Last Glacial Maximum, eastern Himalayan syntaxis. Geomorphology 365, 107246. http://doi.org/10.1016/j.geomorph.2020.107246

Kumar, V., Shukla, T., Mishra, A., Kumar, A., Mehta, M., 2020. Chronology and climate sensitivity of the post-LGM glaciation in the Dunagiri valley, Dhauliganga basin, Central Himalaya, India. Boreas 49, 594-614. http://doi.org/10.1111/bor.12440

Möller, P., Alexanderson, H., Anjar, J., Björck, S., 2020. MIS 3 sediment stratigraphy in southern Sweden sheds new light on the complex glacial history and dynamics across southern Scandinavia. Boreas 49, 389-416. http://doi.org/10.1111/bor.12433

Mueller, D., Preusser, F., Buechi, M.W., Gegg, L., Deplazes, G., 2020. Luminescence properties and dating of glacial to periglacial sediments from northern Switzerland. Geochronology 2, 305-323. http://doi.org/10.5194/gchron-2-305-2020

Muñoz-Salinas, E., Castillo, M., Franco-Ramos, O., Arce, J.L., Sanderson, D.C.W., Cresswell, A.C., 2020. Assessing paraglacial processes at Nexpayantla Gorge (Popocatépetl volcano, Central Mexico) using OSL and 14C. Earth Surface Processes and Landforms 45, 2450-2462. http://doi.org/10.1002/esp.4890

Obst, K., Ansorge, J., Thiel, C., Frenzel, P., 2020. The Late Saalian Cyprina clay of northeastern Germany and the following Weichselian sedimentation and deformation history – Review and new data. Boreas 49, 488-513. http://doi.org/10.1111/bor.12439

Roberts, D.H., Ó Cofaigh, C., Ballantyne, C.K., Burke, M., Chiverrell, R.C., Evans, D.J.A., Clark, C.D., Duller, G.A.T., Ely, J., Fabel, D., Small, D., Smedley, R.K., Callard, S.L., 2020. The deglaciation of the western sector of the Irish Ice Sheet from the inner continental shelf to its terrestrial margin. Boreas 49, 438-460. http://doi.org/10.1111/bor.12448

Saha, S., Owen, L.A., Orr, E.N., Caffee, M.W., 2020. A statistical and numerical modeling approach for spatiotemporal reconstruction of glaciations in the Central Asian mountains. MethodsX 7, 100820. http://doi.org/10.1016/j.mex.2020.100820

Sizov, O., Volvakh, A., Molodkov, A., Vishnevskiy, A., Soromotin, A., Abakumov, E., 2020. Lithological and geomorphological indicators of glacial genesis in the upper Quaternary strata, Nadym River basin, Western Siberia. Solid Earth 11, 2047-2074. http://doi.org/10.5194/se-11-2047-2020

Wolfe, S., Murton, J., Bateman, M., Barlow, J., 2020. Oriented-lake development in the context of late Quaternary landscape evolution, McKinley Bay Coastal Plain, western Arctic Canada. Quaternary Science Reviews 242, 106414. http://doi.org/10.1016/j.quascirev.2020.106414

- lacustrine

Abu-Jaber, N., Al Khasawneh, S., Alqudah, M., Hamarneh, C., Al-Rawabdeh, A., Murray, A., 2020. Lake Elji and a geological perspective on the evolution of Petra, Jordan. Palaeogeography, Palaeoclimatology, Palaeoecology 557, 109904. http://doi.org/10.1016/j.palaeo.2020.109904

Chen, C., Tao, S., Zhao, W., Jin, M., Wang, Z., Li, H., Ren, H., Li, G., 2021. Holocene lake level, vegetation, and climate at the East Asian summer monsoon margin: A record from the Lake Wulanhushao basin, southern Inner Mongolia. Palaeogeography, Palaeoclimatology, Palaeoecology 561, 110051. http://doi.org/10.1016/j.palaeo.2020.110051

Chen, F., Feng, J.-L., Hu, H.-P., Wang, P., 2020. Mid-Holocene palaeohydrochemistry and palaeohydrology of Yamdrok Yumtso, southern Tibetan Plateau, reconstructed from δ18O and δ13C of fossil shells of the gastropod Radix auricularia. The Holocene 30, 1741-1751. http://doi.org/10.1177/0959683620950426

Jonell, T.N., Aitchison, J.C., Li, G., Shulmeister, J., Zhou, R., Zhang, H., 2020. Revisiting growth and decline of late Quaternary mega-lakes across the south-central Tibetan Plateau. Quaternary Science Reviews 248, 106475. http://doi.org/10.1016/j.quascirev.2020.106475

Kaiser, K., Schneider, T., Küster, M., Dietze, E., Fülling, A., Heinrich, S., Kappler, C., Nelle, O., Schult, M., Theuerkauf, M., Vogel, S., de Boer, A.M., Börner, A., Preusser, F., Schwabe, M., Ulrich, J., Wirner, M., Bens, O., 2020. Palaeosols and their cover sediments of a glacial landscape in northern central Europe: Spatial distribution, pedostratigraphy and evidence on landscape evolution. CATENA 193, 104647. http://doi.org/10.1016/j.catena.2020.104647

Ling, Z., Yang, X., Wang, Y., Wang, Y., Jin, J., Zhang, D., Chen, F., 2020. OSL chronology of the Liena archeological site in the Yarlung Tsangpo valley throws new light on human occupation of the Tibetan Plateau. The Holocene 30, 1043-1052. http://doi.org/10.1177/0959683620908643

Liu, X., Hu, J., Shi, W., Chen, H., Liang, X., Li, M., 2020. Stratigraphy and its environmental implications of the Late Pleistocene Shuidonggou Formation in the western Ordos Block, North China. Geological Journal 55, 7359-7370. http://doi.org/10.1002/gj.3972

Munroe, J.S., Walcott, C.K., Amidon, W.H., Landis, J.D., 2020. A top-to-bottom luminescence-based chronology for the post-LGM regression of a great basin pluvial lake. Quaternary 3, 11. http://doi.org/10.3390/quat3020011

Shukla, T., Mehta, M., Dobhal, D.P., Bohra, A., Pratap, B., Kumar, A., 2020. Late-Holocene climate response and glacial fluctuations revealed by the sediment record of the monsoon-dominated Chorabari Lake, Central Himalaya. The Holocene 30, 953-965. http://doi.org/10.1177/0959683620908654

Torabi, M., Fattahi, M., Amini, H., Ghassemi, M.R., Karimi, N., 2020. OSL dating of landslide-dammed-lake deposits in the North of Tehran, Iran: 958 Ray-Taleghan/Ruyan earthquake. Quaternary International 562, 46-57. http://doi.org/10.1016/j.quaint.2020.07.006

Vyse, S.A., Herzschuh, U., Andreev, A.A., Pestryakova, L.A., Diekmann, B., Armitage, S.J., Biskaborn, B.K., 2020. Geochemical and sedimentological responses of arctic glacial Lake Ilirney, chukotka (far east Russia) to palaeoenvironmental change since ~51.8 ka BP. Quaternary Science Reviews 247, 106607. http://doi.org/10.1016/j.quascirev.2020.106607

Yuxin, F., Zhenjun, L., Guangliang, Y., Shuangwen, Y., Qingsong, Z., Wenhao, L., Xuesong, M., 2020. Sedimentary evidence and luminescence and ESR dating of Early Pleistocene high lake levels of Megalake Tengger, northwestern China. Journal of Quaternary Science 35, 994-1006. http://doi.org/10.1002/jqs.3246

- loess

Avram, A., Constantin, D., Veres, D., Kelemen, S., Obreht, I., Hambach, U., Marković, S.B., Timar-Gabor, A., 2020. Testing polymineral post-IR IRSL and quartz SAR-OSL protocols on Middle to Late Pleistocene loess at Batajnica, Serbia. Boreas 49, 615-633. http://doi.org/10.1111/bor.12442

Balescu, S., Jordanova, D., Forget Brisson, L., Hardy, F., Huot, S., Lamothe, M., 2020. Luminescence chronology of the northeastern Bulgarian loess-paleosol sequences (Viatovo and Kaolinovo). Quaternary International 552, 15-24. http://doi.org/10.1016/j.quaint.2019.04.020

Bosq, M., Kreutzer, S., Bertran, P., Degeai, J.-P., Dugas, P., Kadereit, A., Lanos, P., Moine, O., Pfaffner, N., Queffelec, A., Sauer, D., 2020. Chronostratigraphy of two Late Pleistocene loess-palaeosol sequences in the Rhône Valley (southeast France). Quaternary Science Reviews 245, 106473. http://doi.org/10.1016/j.quascirev.2020.106473

Duan, F., An, C., Wang, W., Herzschuh, U., Zhang, M., Zhang, H., Liu, Y., Zhao, Y., Li, G., 2020. Dating of a late Quaternary loess section from the northern slope of the Tianshan Mountains (Xinjiang, China) and its paleoenvironmental significance. Quaternary International 544, 104-112. http://doi.org/10.1016/j.quaint.2020.02.034

Fenn, K., Durcan, J.A., Thomas, D.S.G., Millar, I.L., Marković, S.B., 2020. Re-analysis of late Quaternary dust mass accumulation rates in Serbia using new luminescence chronology for loess–palaeosol sequence at Surduk. Boreas 49, 634-652. http://doi.org/10.1111/bor.12445

Fischer, P., Jöris, O., Fitzsimmons, K.E., Vinnepand, M., Prud'homme, C., Schulte, P., Hatté, C., Hambach, U., Lindauer, S., Zeeden, C., Peric, Z., Lehmkuhl, F., Wunderlich, T., Wilken, D., Schirmer, W., Vött, A., 2021. Millennial-scale terrestrial ecosystem responses to Upper Pleistocene climatic changes: 4D-reconstruction of the Schwalbenberg Loess-Palaeosol-Sequence (Middle Rhine Valley, Germany). CATENA 196, 104913. http://doi.org/10.1016/j.catena.2020.104913

Fitzsimmons, K.E., Doboş, A., Probst, M., Iovita, R., 2020. Thinking outside the box at open-air archeological contexts: Examples from loess landscapes in southeast Romania. Frontiers in Earth Science 8, 561207. http://doi.org/10.3389/feart.2020.561207

Flašarová, K., Strouhalová, B., Šefrna, L., Verrecchia, E., Lauer, T., Juřičková, L., Kolařík, P., Ložek, V., 2020. Multiproxy evidence of middle and Late Pleistocene environmental changes in the loess-paleosol sequence of Bůhzdař (Czech Republic). Quaternary International 552, 4-14. http://doi.org/10.1016/j.quaint.2019.10.004

Kang, S., Wang, X., Roberts, H.M., Duller, G.A.T., Song, Y., Liu, W., Zhang, R., Liu, X., Lan, J., 2020. Increasing effective moisture during the Holocene in the semiarid regions of the Yili Basin, Central Asia: Evidence from loess sections. Quaternary Science Reviews 246, 106553. http://doi.org/10.1016/j.quascirev.2020.106553

Novothny, Á., Barta, G., Végh, T., Bradák, B., Surányi, G., Horváth, E., 2020. Correlation of drilling cores and the Paks brickyard key section at the area of Paks, Hungary. Quaternary International 552, 50-61. http://doi.org/10.1016/j.quaint.2019.09.012

Perić, Z.M., Marković, S.B., Sipos, G., Gavrilov, M.B., Thiel, C., Zeeden, C., Murray, A.S., 2020. A post-IR IRSL chronology and dust mass accumulation rates of the Nosak loess-palaeosol sequence in northeastern Serbia. Boreas 49, 841-857. http://doi.org/10.1111/bor.12459

Richter, M., Tsukamoto, S., Long, H., 2020. ESR dating of Chinese loess using the quartz Ti centre: A comparison with independent age control. Quaternary International 556, 159-164. http://doi.org/10.1016/j.quaint.2019.04.003

Schellmann, G., Schielein, P., Burow, C., Radtke, U., 2020. Accuracy of ESR dating of small gastropods from loess and fluvial deposits in the Bavarian Alpine Foreland. Quaternary International 556, 198-215. http://doi.org/10.1016/j.quaint.2019.07.026

Stevens, T., Sechi, D., Bradák, B., Orbe, R., Baykal, Y., Cossu, G., Tziavaras, C., Andreucci, S., Pascucci, V., 2020. Abrupt last glacial dust fall over southeast England associated with dynamics of the British-Irish ice sheet. Quaternary Science Reviews 250, 106641. http://doi.org/10.1016/j.quascirev.2020.106641

Sycheva, S., Frechen, M., Terhorst, B., Sedov, S., Khokhlova, O., 2020. Pedostratigraphy and chronology of the Late Pleistocene for the extra glacial area in the Central Russian Upland (reference section Aleksandrov quarry). CATENA 194, 104689. http://doi.org/10.1016/j.catena.2020.104689

Tugulan, L., Secu, M., Bercu, V., Cotrubinis, M., Duliu, O.G., 2020. Concordant ESR and TL depositional age of Romanian Plane loess, in: Shukla, A.K. (Ed.), Spectroscopic Techniques for Archaeological and Cultural Heritage Research. IOP Publishing, pp. 1-9. http://doi.org/10.1088/978-0-7503-2616-2ch5

Yang, H., Li, G., Huang, X., Wang, X., Zhang, Y., Jonell, T.N., Jin, M., Chen, C., Zhao, W., Zhang, H., Wang, Z., Deng, Y., 2020. Loess depositional dynamics and paleoclimatic changes in the Yili Basin, Central Asia, over the past 250 ka. CATENA 195, 104881. http://doi.org/10.1016/j.catena.2020.104881

Yang, S., Li, D., Liu, N., Zan, J., Liu, W., Kang, J., Murodov, A., Fang, X., 2020. Quartz optically stimulated luminescence dating of loess in Tajikistan and its paleoclimatic implications for arid Central Asia since the Lateglacial. Palaeogeography, Palaeoclimatology, Palaeoecology 556, 109881. http://doi.org/10.1016/j.palaeo.2020.109881

- soil

Dreibrodt, S., Hofmann, R., Sipos, G., Schwark, L., Videiko, M., Shatilo, L., Martini, S., Saggau, P., Bork, H.-R., Kirleis, W., Duttmann, R., Müller, J., 2020. Holocene soil erosion in Eastern Europe-land use and/or climate controlled? The example of a catchment at the Giant Chalcolithic settlement at Maidanetske, central Ukraine. Geomorphology 367, 107302. http://doi.org/10.1016/j.geomorph.2020.107302

Follett, R.F., Stewart, C.E., Bradford, J., Pruessner, E.G., Sims, P.L., Vigil, M.F., 2020. Long-term pasture management impacts on eolian sand soils in the southern mixed-grass prairie. Quaternary International 565, 84-93. http://doi.org/10.1016/j.quaint.2020.07.019

Sycheva, S., Frechen, M., Terhorst, B., Sedov, S., Khokhlova, O., 2020. Pedostratigraphy and chronology of the Late Pleistocene for the extra glacial area in the Central Russian Upland (reference section Aleksandrov quarry). CATENA 194, 104689. http://doi.org/10.1016/j.catena.2020.104689

Wei, H., E, C., Zhang, J., Sun, Y., Li, Q., Hou, G., Duan, R., 2020. Climate change and anthropogenic activities in Qinghai Lake basin over the last 8500 years derived from pollen and charcoal records in an aeolian section. CATENA 193, 104616. http://doi.org/10.1016/j.catena.2020.104616

Zhang, J., E, C., Wu, C., Sun, Y., Li, P., Shi, Y., Sun, M., 2020. An alpine meadow soil chronology based on OSL and radiocarbon dating, Qinghai Lake, northeastern Tibetan Plateau. Quaternary International 562, 35-45. http://doi.org/10.1016/j.quaint.2020.05.044

- surface exposure dating

Brown, N.D., 2020. Which geomorphic processes can be informed by luminescence measurements? Geomorphology 367, 107296. http://doi.org/10.1016/j.geomorph.2020.107296

Stange, K.M., Midtkandal, I., Nystuen, J.P., Murray, A., Sohbati, R., Thompson, W., Spiegel, C., Kuss, H.-J., 2019. Erosive response of non-glaciated Pyrenean headwater catchments to the last major climate transition and establishing interglacial conditions. Quaternary 2, 17. http://doi.org/10.3390/quat2020017

- thermochronology

Pagonis, V., Kitis, G., Polymeris, G.S., 2020. Quantum tunneling processes in feldspars: Using thermoluminescence signals in thermochronometry. Radiation Measurements 134, 106325. http://doi.org/10.1016/j.radmeas.2020.106325

Archaeology applications

Aubry, T., Dimuccio, L.A., Barbosa, A.F., Luís, L., Santos, A.T., Silvestre, M., Thomsen, K.J., Rades, E., Autzen, M., Murray, A.S., 2020. Timing of the Middle-to-Upper Palaeolithic transition in the Iberian inland (Cardina-Salto do Boi, Côa Valley, Portugal). Quaternary Research 98, 81-101. http://doi.org/10.1017/qua.2020.43

Azevedo, R.L., Asfora, V.K., Mützenberg, D.S., Cisneiros, D., Sullasi, H.L., Kinoshita, A.M., Guzzo, P.L., Skinner, A.R., Baffa, O., Pessis, A.-M., Khoury, H.J., 2020. ESR dating of megafauna enamel teeth from

Lagoa Uri de Cima Archaeological Site (Pernambuco, Northeastern Brazil). Quaternary International 556, 38-48. http://doi.org/10.1016/j.quaint.2019.02.039

Bahain, J.-J., Duval, M., Voinchet, P., Tissoux, H., Falguères, C., Grün, R., Moreno, D., Shao, Q., Tombret, O., Jamet, G., Faivre, J.-P., Cliquet, D., 2020. ESR and ESR/U-series chronology of the Middle Pleistocene site of Tourville-la-Rivière (Normandy, France) - A multi-laboratory approach. Quaternary International 556, 58-70. http://doi.org/10.1016/j.quaint.2019.06.015

Ben Arous, E., Falguères, C., Tombret, O., El Hajraoui, M.A., Nespoulet, R., 2020. Combined US-ESR dating of fossil teeth from El Harhoura 2 cave (Morocco): New data about the end of the MSA in Temara region. Quaternary International 556, 88-95. http://doi.org/10.1016/j.quaint.2019.02.029

Benito-Calvo, A., Arnold, L.J., Mora, R., Martínez-Moreno, J., Demuro, M., 2020. Reconstructing Mousterian landscapes in the southeastern Pyrenees (Roca dels Bous site, Pre-Pyrenees ranges, Spain). Quaternary Research 97, 167-186. http://doi.org/10.1017/qua.2020.29

de Souza, J.J.L.L., de Souza, B.I., Xavier, R.A., Pacheco, A.A., Pessenda, L.C.R., dos Santos Brito, E., 2020. Archaeoanthrosol formation in the Brazilian semiarid. CATENA 193, 104603. http://doi.org/10.1016/j.catena.2020.104603

Demuro, M., Arnold, L.J., Duval, M., Méndez-Quintas, E., Santonja, M., Pérez-González, A., 2020. Refining the chronology of Acheulean deposits at Porto Maior in the River Miño basin (Galicia, Spain) using a comparative luminescence and ESR dating approach. Quaternary International 556, 96-112. http://doi.org/10.1016/j.quaint.2020.01.005

Duval, M., Voinchet, P., Arnold, L.J., Parés, J.M., Minnella, W., Guilarte, V., Demuro, M., Falguères, C., Bahain, J.-J., Despriée, J., 2020. A multi-technique dating study of two Lower Palaeolithic sites from the Cher Valley (Middle Loire Catchment, France): Lunery-la Terre-des-Sablons and Brinay-la Noira. Quaternary International 556, 71-87. http://doi.org/10.1016/j.quaint.2020.05.033

Falguères, C., 2020. The first human settlements out africa into Europe: A chronological perspective. Quaternary Science Reviews 247, 106551. http://doi.org/10.1016/j.quascirev.2020.106551

Fitzsimmons, K.E., Doboş, A., Probst, M., Iovita, R., 2020. Thinking outside the box at open-air archeological contexts: Examples from loess landscapes in southeast Romania. Frontiers in Earth Science 8, 561207. http://doi.org/10.3389/feart.2020.561207

Forget Brisson, L., Lamothe, M., Hardy, F., Graf, K.E., 2020. Exploring the use of a low temperature preheat in IRSL dating of feldspar in Beringian archaeological contexts. Radiation Measurements 136, 106387. http://doi.org/10.1016/j.radmeas.2020.106387

Guilarte, V., 2020. ESR dating in Archaeology, in: Shukla, A.K. (Ed.), Spectroscopic Techniques for Archaeological and Cultural Heritage Research. IOP Publishing, pp. 1-29. http://doi.org/10.1088/978-0-7503-2616-2ch2

Hein, M., Weiss, M., Otcherednoy, A., Lauer, T., 2020. Luminescence chronology of the key-Middle Paleolithic site Khotylevo I (Western Russia) - Implications for the timing of occupation, site formation and landscape evolution. Quaternary Science Advances 2, 100008. http://doi.org/10.1016/j.qsa.2020.100008

Hornak, J.P., 2020. The development of low frequency EPR spectroscopy for studying objects with cultural heritage significance, in: Shukla, A.K. (Ed.), Spectroscopic Techniques for Archaeological and Cultural Heritage Research. IOP Publishing, pp. 1-60. http://doi.org/10.1088/978-0-7503-2616-2ch3

Hu, G., Wang, P., Rahman, S.M., Li, D., Alam, M.M., Zhang, J., Jin, Z., Fan, A., Chen, J., Zhang, A., Yang, W., 2020. Vicissitudes experienced by the oldest urban center in Bangladesh in relation to the migration of the Brahmaputra River. Journal of Quaternary Science 35, 1089-1099. http://doi.org/10.1002/jqs.3240

Karimi Moayed, N., Vandenberghe, D.A.G., Deforce, K., Bastiaens, J., Ghyselbrecht, E., Debeer, A.E., De Smedt, P., De Clercq, W., De Grave, J., 2020. Bypassing the Suess-effect: Age determination of charcoal kiln remains using OSL dating. Journal of Archaeological Science 120, 105176. http://doi.org/10.1016/j.jas.2020.105176

Langewitz, T., Fülling, A., Klamm, M., Wiedner, K., 2020. Historical classification of ridge and furrow cultivation at selected locations in Northern and central Germany using a multi-dating approach and historical sources. Journal of Archaeological Science 123, 105248. http://doi.org/10.1016/j.jas.2020.105248

Ling, Z., Yang, X., Wang, Y., Wang, Y., Jin, J., Zhang, D., Chen, F., 2020. OSL chronology of the Liena archeological site in the Yarlung Tsangpo valley throws new light on human occupation of the Tibetan Plateau. The Holocene 30, 1043-1052. http://doi.org/10.1177/0959683620908643

Munyikwa, K., Gilliland, K., Plumb, E., Gibson, T., 2020. Investigating post-depositional sediment mixing at an archaeological site on the northern Plains using a portable optically stimulated luminescence (OSL) reader. Journal of Archaeological Science: Reports 33, 102508. http://doi.org/10.1016/j.jasrep.2020.102508

Niang, K., Blinkhorn, J., Ndiaye, M., Bateman, M., Seck, B., Sawaré, G., 2020. The Middle Stone Age occupations of Tiémassas, coastal West Africa, between 62 and 25 thousand years ago. Journal of Archaeological Science: Reports 34, 102658. http://doi.org/10.1016/j.jasrep.2020.102658

Ochando, J., Carrión, J.S., Blasco, R., Rivals, F., Rufà, A., Demuro, M., Arnold, L.J., Amorós, G., Munuera, M., Fernández, S., Rosell, J., 2020. Neanderthals in a highly diverse, mediterranean-Eurosiberian forest ecotone: The pleistocene pollen record of Teixoneres Cave, northeastern Spain. Quaternary Science Reviews 241, 106429. http://doi.org/10.1016/j.quascirev.2020.106429

Panzeri, L., Maspero, F., Galli, A., Sibilia, E., Martini, M., 2020. Luminescence and Radiocarbon Dating of Mortars at Milano-Bicocca Laboratories. Radiocarbon 62, 657-666. http://doi.org/10.1017/RDC.2020.6

Richard, M., Falguères, C., Pons-Branchu, E., Richter, D., Beutelspacher, T., Conard, N.J., Kind, C.J., 2020. The Middle to Upper Palaeolithic transition in Hohlenstein-Stadel cave (Swabian Jura, Germany): A comparison between ESR, U-series and radiocarbon dating. Quaternary International 556, 49-57. http://doi.org/10.1016/j.quaint.2019.04.009

Saos, T., Grégoire, S., Bahain, J.-J., Higham, T., Moigne, A.-M., Testu, A., Boulbes, N., Bachellerie, M., Chevalier, T., Becam, G., Duran, J.-P., Alladio, A., Ortega, M.I., Devièse, T., Shao, Q., 2020. The Middle and Upper Palaeolithic at La Crouzade cave (Gruissan, Aude, France): New excavations and a chronostratigraphic framework. Quaternary International 551, 85-104. http://doi.org/10.1016/j.quaint.2019.11.040

Stewart, M., Clark-Wilson, R., Breeze, P.S., Janulis, K., Candy, I., Armitage, S.J., Ryves, D.B., Louys, J., Duval, M., Price, G.J., Cuthbertson, P., Bernal, M.A., Drake, N.A., Alsharekh, A.M., Zahrani, B., Al-Omari, A., Roberts, P., Groucutt, H.S., Petraglia, M.D., 2020. Human footprints provide snapshot of last interglacial ecology in the Arabian interior. Science Advances 6, eaba8940. http://doi.org/10.1126/sciadv.aba8940

Tirelli, G., Lugli, S., Galli, A., Hajdas, I., Lindroos, A., Martini, M., Maspero, F., Olsen, J., Ringbom, Å., Sibilia, E., Caroselli, M., Silvestri, E., Panzeri, L., 2020. Integrated Dating of the Construction and Restoration of the Modena Cathedral Vaults (Northern Italy): Preliminary Results. Radiocarbon 62, 667-677. http://doi.org/10.1017/RDC.2020.10

Toyoda, S., 2020. Determination by ESR of the temperature of prehistoric lithic heat treatment, in: Shukla, A.K. (Ed.), Spectroscopic Techniques for Archaeological and Cultural Heritage Research. IOP Publishing, pp. 1-13. http://doi.org/10.1088/978-0-7503-2616-2ch4

Walker, M.J., Haber Uriarte, M., López Jiménez, A., López Martínez, M., Martín Lerma, I., Van der Made, J., Duval, M., Grün, R., 2020. Cueva Negra del Estrecho del Río Quípar: a Dated Late Early Pleistocene Palaeolithic Site in Southeastern Spain. Journal of Paleolithic Archaeologyhttp://doi.org/10.1007/s41982-020-00062-5

Xiaoqi, G., Xuefeng, S., Xiaobo, F., Shuangwen, Y., Xinying, Z., Deyin, L., Qiqi, T., 2020. Luminescence dating of the Jigongshan Paleolithic site in Hubei Province, southern China. Quaternary International 554, 36-44. http://doi.org/10.1016/j.quaint.2020.08.014

Yao, Y., Liao, W., Bae, C.J., Sun, X., Feng, Y., Tian, C., Li, J., Wei, S., Wang, W., 2020. New discovery of Late Pleistocene modern human teeth from Chongzuo, Guangxi, southern China. Quaternary International 563, 5-12. http://doi.org/10.1016/j.quaint.2020.02.002

Zeitoun, V., Chinnawut, W., Arnaud, L., Bochaton, C., Burdette, K., Thompson, J., Mallye, J.-B., Frère, S., Debruyne, R., Antoine, P.-O., William, J.R., Prasit, A., 2019. Dating, stratigraphy and taphonomy of the Pleistocene site of Ban Fa Suai II (Northern Thailand): Contributions to the study of paleobiodiversity in Southeast Asia. Annales de Paléontologie 105, 275-285. http://doi.org/10.1016/j.annpal.2019.03.005

Various ESR applications

Azevedo, R.L., Asfora, V.K., Mützenberg, D.S., Cisneiros, D., Sullasi, H.L., Kinoshita, A.M., Guzzo, P.L., Skinner, A.R., Baffa, O., Pessis, A.-M., Khoury, H.J., 2020. ESR dating of megafauna enamel teeth from Lagoa Uri de Cima Archaeological Site (Pernambuco, Northeastern Brazil). Quaternary International 556, 38-48. http://doi.org/10.1016/j.quaint.2019.02.039

Bahain, J.-J., Duval, M., Voinchet, P., Tissoux, H., Falguères, C., Grün, R., Moreno, D., Shao, Q., Tombret, O., Jamet, G., Faivre, J.-P., Cliquet, D., 2020. ESR and ESR/U-series chronology of the Middle Pleistocene site of Tourville-la-Rivière (Normandy, France) - A multi-laboratory approach. Quaternary International 556, 58-70. http://doi.org/10.1016/j.quaint.2019.06.015

Bartz, M., Duval, M., Brill, D., Zander, A., King, G.E., Rhein, A., Walk, J., Stauch, G., Lehmkuhl, F., Brückner, H., 2020. Testing the potential of K-feldspar pIR-IRSL and quartz ESR for dating coastal alluvial fan

complexes in arid environments. Quaternary International 556, 124-143. http://doi.org/10.1016/j.quaint.2020.03.037

Beerten, K., Verbeeck, K., Laloy, E., Vanacker, V., Vandenberghe, D., Christl, M., De Grave, J., Wouters, L., 2020. Electron spin resonance (ESR), optically stimulated luminescence (OSL) and terrestrial cosmogenic radionuclide (TCN) dating of quartz from a Plio-Pleistocene sandy formation in the Campine area, NE Belgium. Quaternary International 556, 144-158. http://doi.org/10.1016/j.quaint.2020.06.011

Ben Arous, E., Falguères, C., Tombret, O., El Hajraoui, M.A., Nespoulet, R., 2020. Combined US-ESR dating of fossil teeth from El Harhoura 2 cave (Morocco): New data about the end of the MSA in Temara region. Quaternary International 556, 88-95. http://doi.org/10.1016/j.quaint.2019.02.029

Demuro, M., Arnold, L.J., Duval, M., Méndez-Quintas, E., Santonja, M., Pérez-González, A., 2020. Refining the chronology of Acheulean deposits at Porto Maior in the River Miño basin (Galicia, Spain) using a comparative luminescence and ESR dating approach. Quaternary International 556, 96-112. http://doi.org/10.1016/j.quaint.2020.01.005

Demuro, M., Duval, M., Arnold, L.J., Spooner, N.A., Creighton, D.F., Méndez-Quintas, E., Santonja, M., Pérez-González, A., 2020. Insights into the relationship between luminescence and ESR dating signals from Spanish sedimentary quartz samples of different geologic origins. Quaternary International 556, 165-179. http://doi.org/10.1016/j.quaint.2020.05.037

Duval, M., Arnold, L.J., Rixhon, G., 2020. Electron spin resonance (ESR) dating in Quaternary studies: evolution, recent advances and applications. Quaternary International 556, 1-10. http://doi.org/10.1016/j.quaint.2020.07.044

Duval, M., Voinchet, P., Arnold, L.J., Parés, J.M., Minnella, W., Guilarte, V., Demuro, M., Falguères, C., Bahain, J.-J., Despriée, J., 2020. A multi-technique dating study of two Lower Palaeolithic sites from the Cher Valley (Middle Loire Catchment, France): Lunery-la Terre-des-Sablons and Brinay-la Noira. Quaternary International 556, 71-87. http://doi.org/10.1016/j.quaint.2020.05.033

Falguères, C., 2020. A French story of the ESR dating method for Quaternary samples. Quaternary International 556, 11-19. http://doi.org/10.1016/j.quaint.2019.09.047

Grün, R., 2020. A very personal, 35 years long journey in ESR dating. Quaternary International 556, 20-37. http://doi.org/10.1016/j.quaint.2018.11.038

Guilarte, V., 2020. ESR dating in Archaeology, in: Shukla, A.K. (Ed.), Spectroscopic Techniques for Archaeological and Cultural Heritage Research. IOP Publishing, pp. 1-29. http://doi.org/10.1088/978-0-7503-2616-2ch2

Hornak, J.P., 2020. The development of low frequency EPR spectroscopy for studying objects with cultural heritage significance, in: Shukla, A.K. (Ed.), Spectroscopic Techniques for Archaeological and Cultural Heritage Research. IOP Publishing, pp. 1-60. http://doi.org/10.1088/978-0-7503-2616-2ch3

Hu, C., Li, W., Cao, L., Xu, G., Zhou, Y., 2019. Evidence for wetter climate recorded in the Jingxian red clay section since approximately 840 ka ago and its relationship with the East Asian summer monsoon intensity. Quaternary International 532, 57-65. http://doi.org/10.1016/j.quaint.2019.09.031

Marra, F., Bahain, J.-J., Jicha, B.R., Nomade, S., Palladino, D.M., Pereira, A., Tolomei, C., Voinchet, P., Anzidei, M., Aureli, D., Ceruleo, P., Falguères, C., Florindo, F., Gatta, M., Ghaleb, B., La Rosa, M., Peretto, C., Petronio, C., Rocca, R., Rolfo, M.F., Salari, L., Smedile, A., Tombret, O., 2019. Reconstruction of the MIS 5.5, 5.3 and 5.1 coastal terraces in Latium (central Italy): A re-evaluation of the sea-level history in the Mediterranean Sea during the last interglacial. Quaternary International 525, 54-77. http://doi.org/10.1016/j.quaint.2019.09.001

Molodkov, A., 2020. The Late Pleistocene palaeoenvironmental evolution in Northern Eurasia through the prism of the mollusc shell-based ESR dating evidence. Quaternary International 556, 180-197. http://doi.org/10.1016/j.quaint.2019.05.031

Oka, T., Takahashi, A., Koarai, K., Mitsuyasu, Y., Kino, Y., Sekine, T., Shimizu, Y., Chiba, M., Suzuki, T., Osaka, K., Sasaki, K., Urushihara, Y., Endo, S., Suzuki, M., Shinoda, H., Fukumoto, M., 2020. External exposure dose estimation by electron spin resonance technique for wild Japanese macaque captured in Fukushima Prefecture. Radiation Measurements 134, 106315. http://doi.org/10.1016/j.radmeas.2020.106315

Rashad, A.M., Helal, A.E.I., Ahmed, G., Kassem, S., Fahim, R., Salem, S., Mohamed, S.E.-D., Gamal, A., 2020. Spectroscopic analysis of irradiated natural quartz and ESR dating aspects. Arab Journal of Nuclear Sciences and Applications 53, 197-209. http://doi.org/10.21608/ajnsa.2020.22502.1321

Richard, M., Falguères, C., Pons-Branchu, E., Richter, D., Beutelspacher, T., Conard, N.J., Kind, C.J., 2020. The Middle to Upper Palaeolithic transition in Hohlenstein-Stadel cave (Swabian Jura, Germany): A comparison between ESR, U-series and radiocarbon dating. Quaternary International 556, 49-57. http://doi.org/10.1016/j.quaint.2019.04.009

Richter, M., Tsukamoto, S., Long, H., 2020. ESR dating of Chinese loess using the quartz Ti centre: A comparison with independent age control. Quaternary International 556, 159-164. http://doi.org/10.1016/j.quaint.2019.04.003

Saos, T., Grégoire, S., Bahain, J.-J., Higham, T., Moigne, A.-M., Testu, A., Boulbes, N., Bachellerie, M., Chevalier, T., Becam, G., Duran, J.-P., Alladio, A., Ortega, M.I., Devièse, T., Shao, Q., 2020. The Middle and Upper Palaeolithic at La Crouzade cave (Gruissan, Aude, France): New excavations and a chronostratigraphic framework. Quaternary International 551, 85-104. http://doi.org/10.1016/j.quaint.2019.11.040

Schellmann, G., Schielein, P., Burow, C., Radtke, U., 2020. Accuracy of ESR dating of small gastropods from loess and fluvial deposits in the Bavarian Alpine Foreland. Quaternary International 556, 198-215. http://doi.org/10.1016/j.quaint.2019.07.026

Schielein, P., Burow, C., Pajon, J., Rojas Consuegra, R., Zhao, J.-x., Schellmann, G., 2020. ESR and U-Th dating results for Last Interglacial coral reef terraces at the northern coast of Cuba. Quaternary International 556, 216-229. http://doi.org/10.1016/j.quaint.2019.11.041

Stewart, M., Clark-Wilson, R., Breeze, P.S., Janulis, K., Candy, I., Armitage, S.J., Ryves, D.B., Louys, J., Duval, M., Price, G.J., Cuthbertson, P., Bernal, M.A., Drake, N.A., Alsharekh, A.M., Zahrani, B., Al-Omari, A., Roberts, P., Groucutt, H.S., Petraglia, M.D., 2020. Human footprints provide snapshot of last interglacial ecology in the Arabian interior. Science Advances 6, eaba8940. http://doi.org/10.1126/sciadv.aba8940

Todaka, A., Toyoda, S., Natsuhori, M., Okada, K., Sato, I., Sato, H., Sasaki, J., 2020. ESR assessment of tooth enamel dose from cattle bred in areas contaminated due to the Fukushima Dai-ichi nuclear power plant accident. Radiation Measurements 136, 106357. http://doi.org/10.1016/j.radmeas.2020.106357

Toyoda, S., 2020. Determination by ESR of the temperature of prehistoric lithic heat treatment, in: Shukla, A.K. (Ed.), Spectroscopic Techniques for Archaeological and Cultural Heritage Research. IOP Publishing, pp. 1-13. http://doi.org/10.1088/978-0-7503-2616-2ch4

Toyoda, S., Murahashi, M., Ivannikov, A., 2020. ESR tooth enamel retrospective dosimetry quoted as spin numbers. Radiation Measurements 135, 106333. http://doi.org/10.1016/j.radmeas.2020.106333

Tugulan, L., Secu, M., Bercu, V., Cotrubinis, M., Duliu, O.G., 2020. Concordant ESR and TL depositional age of Romanian Plane loess, in: Shukla, A.K. (Ed.), Spectroscopic Techniques for Archaeological and Cultural Heritage Research. IOP Publishing, pp. 1-9. http://doi.org/10.1088/978-0-7503-2616-2ch5

Voinchet, P., Pereira, A., Nomade, S., Falguères, C., Biddittu, I., Piperno, M., Moncel, M.H., Bahain, J.J., 2020. ESR dating applied to optically bleached quartz - A comparison with 40Ar/39Ar chronologies on Italian Middle Pleistocene sequences. Quaternary International 556, 113-123. http://doi.org/10.1016/j.quaint.2020.03.012

Walker, M.J., Haber Uriarte, M., López Jiménez, A., López Martínez, M., Martín Lerma, I., Van der Made, J., Duval, M., Grün, R., 2020. Cueva Negra del Estrecho del Río Quípar: a Dated Late Early Pleistocene Palaeolithic Site in Southeastern Spain. Journal of Paleolithic Archaeologyhttp://doi.org/10.1007/s41982-020-00062-5

Yuxin, F., Zhenjun, L., Guangliang, Y., Shuangwen, Y., Qingsong, Z., Wenhao, L., Xuesong, M., 2020. Sedimentary evidence and luminescence and ESR dating of Early Pleistocene high lake levels of Megalake Tengger, northwestern China. Journal of Quaternary Science 35, 994-1006. http://doi.org/10.1002/jqs.3246

Zeitoun, V., Chinnawut, W., Arnaud, L., Bochaton, C., Burdette, K., Thompson, J., Mallye, J.-B., Frère, S., Debruyne, R., Antoine, P.-O., William, J.R., Prasit, A., 2019. Dating, stratigraphy and taphonomy of the Pleistocene site of Ban Fa Suai II (Northern Thailand): Contributions to the study of paleobiodiversity in Southeast Asia. Annales de Paléontologie 105, 275-285. http://doi.org/10.1016/j.annpal.2019.03.005

Zhang, D., Wang, G., Pullen, A., Abell, J.T., Ji, J., Shen, T., 2020. Landscape evolution and development of eolian-modified unconsolidated gravel surfaces and yardangs in the Hami Basin, China. Geomorphology 368, 107355. http://doi.org/10.1016/j.geomorph.2020.107355

Basic research

Angeli, V., Kitis, G., Pagonis, V., Polymeris, G.S., 2020. Sequential two-step optical stimulation in K-feldspars: Correlation among the luminescence signals and implications for modeling parameters. Journal of Luminescence 226, 117425. http://doi.org/10.1016/j.jlumin.2020.117425

Autzen, M., Hansen, V., Murray, A.S., 2020. Reply to "Further considerations on 'Towards the origins of over-dispersion in beta source calibration' by Hansen et al., radiation measurements, 2018" by Munish Kumar. Radiation Measurements 138, 106446. http://doi.org/10.1016/j.radmeas.2020.106446

Brown, N.D., 2020. Which geomorphic processes can be informed by luminescence measurements? Geomorphology 367, 107296. http://doi.org/10.1016/j.geomorph.2020.107296

Chen, R., Lawless, J.L., Pagonis, V., 2020. Competition between long time excitation and fading of thermoluminescence (TL) and optically stimulated luminescence (OSL). Radiation Measurements 136, 106422. http://doi.org/10.1016/j.radmeas.2020.106422

Chruścińska, A., Palczewski, P., Rerek, T., 2020. Slow OSL component in quartz separated by TM-OSL method. Radiation Measurements 134, 106316. http://doi.org/10.1016/j.radmeas.2020.106316

Chruścińska, A., Palczewski, P., Rerek, T., Biernacka, M., Lefrais, Y., 2021. Measurement of the paleodose in luminescence dating using the TM-OSL of quartz. Measurement 167, 108448. http://doi.org/10.1016/j.measurement.2020.108448

Colarossi, D., Duller, G.A.T., Roberts, H.M., Tooth, S., Botha, G.A., 2020. A comparison of multiple luminescence chronometers at Voordrag, South Africa. Quaternary Geochronology 60, 101094. http://doi.org/10.1016/j.quageo.2020.101094

Fu, X., Li, B., Jacobs, Z., Jankowski, N.R., Cohen, T.J., Roberts, R.G., 2020. Establishing standardised growth curves (SGCs) for OSL signals from individual grains of quartz: A continental-scale case study. Quaternary Geochronology 60, 101107. http://doi.org/10.1016/j.quageo.2020.101107

Jain, M., Kumar, R., Kook, M., 2020. A novel coupled RPL/OSL system to understand the dynamics of the metastable states. Scientific Reports 10, 15565. http://doi.org/10.1038/s41598-020-72434-4

Kalita, J.M., Chithambo, M.L., 2021. Blue- and infrared-light stimulated luminescence of microcline and the effect of optical bleaching on its thermoluminescence. Journal of Luminescence 229, 117712. http://doi.org/10.1016/j.jlumin.2020.117712

Lawless, J.L., Chen, R., Pagonis, V., 2020. Inherent statistics of glow curves from small samples and single grains. Journal of Luminescence 226, 117389. http://doi.org/10.1016/j.jlumin.2020.117389

Mandowska, E., Majgier, R., Mandowski, A., 2020. Influence of optical bleaching on spectrally resolved thermoluminescence in beta irradiated potassium chloride pellets. Radiation Physics and Chemistry 173, 108876. http://doi.org/10.1016/j.radphyschem.2020.108876

Merezhnikov, A.S., Nikiforov, S.V., Pagonis, V., 2020. Simulation of thermoluminescence dose response in cluster systems with deep traps. Radiation Measurements 134, 106307. http://doi.org/10.1016/j.radmeas.2020.106307

Pagonis, V., Kitis, G., Chen, R., 2020. Superlinearity revisited: A new analytical equation for the dose response of defects in solids, using the Lambert W function. Journal of Luminescence 227, 117553. http://doi.org/10.1016/j.jlumin.2020.117553

Pagonis, V., Kitis, G., Polymeris, G.S., 2020. Quantum tunneling processes in feldspars: Using thermoluminescence signals in thermochronometry. Radiation Measurements 134, 106325. http://doi.org/10.1016/j.radmeas.2020.106325

Peng, J., Li, B., Jacobs, Z., 2020. Modelling heterogeneously bleached single-grain equivalent dose distributions: Implications for the reliability of burial dose determination. Quaternary Geochronology 60, 101108. http://doi.org/10.1016/j.quageo.2020.101108

Peng, J., Wang, X., 2020. On the production of the medium component in quartz OSL: Experiments and simulations. Radiation Measurements 138, 106448. http://doi.org/10.1016/j.radmeas.2020.106448

Polymeris, G.S., 2020. Optimization of OSL/IRSL experimental measurement parameters on various types of naturally occurring CaSO4 samples; sensitization pattern versus temperature, bleaching properties and slurry zeroing effect. Nuclear Instruments and Methods in Physics Research Section B: Beam Interactions with Materials and Atoms 480, 38-44. http://doi.org/10.1016/j.nimb.2020.08.004

Rajapara, H.M., Kumar, V., Chauhan, N., Gajjar, P.N., Singhvi, A.K., 2020. Bleaching of blue light stimulated luminescence of quartz by moonlight. Journal of Earth System Science 129, 212. http://doi.org/10.1007/s12040-020-01474-1

Skuja, L., Ollier, N., Kajihara, K., 2020. Luminescence of non-bridging oxygen hole centers as a marker of particle irradiation of α-quartz. Radiation Measurements 135, 106373. http://doi.org/10.1016/j.radmeas.2020.106373

Tudyka, K., Bluszcz, A., Poręba, G., Miłosz, S., Adamiec, G., Kolarczyk, A., Kolb, T., Lomax, J., Fuchs, M., 2020. Increased dose rate precision in combined α and β counting in the μDose system - a probabilistic approach to data analysis. Radiation Measurements 134, 106310. http://doi.org/10.1016/j.radmeas.2020.106310

Van der Heggen, D., Vandenberghe, D., Moayed, N.K., De Grave, J., Smet, P.F., Joos, J.J., 2020. The almost hidden role of deep traps when measuring afterglow and thermoluminescence of persistent phosphors. Journal of Luminescence 226, 117496. http://doi.org/10.1016/j.jlumin.2020.117496

Yin, L., Townsend, P., Wang, Y., Reza Khanlary, M., Yang, M., 2020. Comparisons of thermoluminescence signals between crystal and powder samples. Radiation Measurements 135, 106380. http://doi.org/10.1016/j.radmeas.2020.106380

Dose rate issues

Tudyka, K., Bluszcz, A., Poręba, G., Miłosz, S., Adamiec, G., Kolarczyk, A., Kolb, T., Lomax, J., Fuchs, M., 2020. Increased dose rate precision in combined α and β counting in the μDose system - a probabilistic approach to data analysis. Radiation Measurements 134, 106310. http://doi.org/10.1016/j.radmeas.2020.106310

Dosimetry

Bassinet, C., Le Bris, W., 2020. TL investigation of glasses from mobile phone screen protectors for radiation accident dosimetry. Radiation Measurements 136, 106384. http://doi.org/10.1016/j.radmeas.2020.106384

Bossin, L., Bailiff, I., Terry, I., 2020. Radiological emergency dosimetry – The use of luminescent mineral fillers in polymer-based fabrics. Radiation Measurements 134, 106318. http://doi.org/10.1016/j.radmeas.2020.106318

Goto, S., Hayashi, H., Asahara, T., Kimoto, N., Tomita, E., Takegami, K., Asakawa, T., Kanazawa, Y., Okazaki, T., Hashizume, T., 2020. An idea to reduce angular dependence of dosimeter having a disk-shaped detection region. Radiation Measurements 137, 106323. http://doi.org/10.1016/j.radmeas.2020.106323

Kim, H., Kim, M.C., Lee, J., Discher, M., Woda, C., Lim, S., Chang, I., Lee, S.K., Kim, J.-L., Chung, K., 2020. Characterization of thermoluminescence of chip cards for emergency dosimetry. Radiation Measurements 134, 106321. http://doi.org/10.1016/j.radmeas.2020.106321

Mafodda, A., Woda, C., 2020. External dose-rate measurements based on smartphone CMOS sensors. Radiation Measurements 137, 106403. http://doi.org/10.1016/j.radmeas.2020.106403

Mandowska, E., Majgier, R., Mandowski, A., 2020. Influence of optical bleaching on spectrally resolved thermoluminescence in beta irradiated potassium chloride pellets. Radiation Physics and Chemistry 173, 108876. http://doi.org/10.1016/j.radphyschem.2020.108876

Mentzel, F., Kröninger, K., Röhrig, L., Speicher, L., Steil, M.-L., Theinert, R., Walbersloh, J., 2020. Extending information relevant for personal dose monitoring obtained from glow curves of thermoluminescence dosimeters using artificial neural networks. Radiation Measurements 136, 106375. http://doi.org/10.1016/j.radmeas.2020.106375

Mrozik, A., Bilski, P., Gieszczyk, W., Zorenko, Y., Gorbenko, V., 2020. Investigations of the influence of Am-241 photons on the measured alpha particle response of luminescent materials. Radiation Measurements 134, 106331. http://doi.org/10.1016/j.radmeas.2020.106331

Ogundare, F.O., Chithambo, M.L., Akintunde, B.O., 2021. Optically stimulated luminescence of cowrie shells. Applied Radiation and Isotopes 167, 109463. http://doi.org/10.1016/j.apradiso.2020.109463

Oka, T., Takahashi, A., Koarai, K., Mitsuyasu, Y., Kino, Y., Sekine, T., Shimizu, Y., Chiba, M., Suzuki, T., Osaka, K., Sasaki, K., Urushihara, Y., Endo, S., Suzuki, M., Shinoda, H., Fukumoto, M., 2020. External exposure dose estimation by electron spin resonance technique for wild Japanese macaque captured in Fukushima Prefecture. Radiation Measurements 134, 106315. http://doi.org/10.1016/j.radmeas.2020.106315

Sholom, S., McKeever, S.W.S., Chandler, J.R., 2020. OSL dosimetry with protective glasses of modern smartphones: A fiber-optic, non-destructive approach. Radiation Measurements 136, 106382. http://doi.org/10.1016/j.radmeas.2020.106382

Shrestha, N., Yukihara, E.G., Cusumano, D., Placidi, L., 2020. Al2O3:C and Al2O3:C,Mg optically stimulated luminescence 2D dosimetry applied to magnetic resonance guided radiotherapy. Radiation Measurements 138, 106439. http://doi.org/10.1016/j.radmeas.2020.106439

Todaka, A., Toyoda, S., Natsuhori, M., Okada, K., Sato, I., Sato, H., Sasaki, J., 2020. ESR assessment of tooth enamel dose from cattle bred in areas contaminated due to the Fukushima Dai-ichi nuclear power plant accident. Radiation Measurements 136, 106357. http://doi.org/10.1016/j.radmeas.2020.106357

Toyoda, S., Murahashi, M., Ivannikov, A., 2020. ESR tooth enamel retrospective dosimetry quoted as spin numbers. Radiation Measurements 135, 106333. http://doi.org/10.1016/j.radmeas.2020.106333

Trindade, N.M., Cruz, M.R., Yoshimura, E.M., 2020. Correlation between thermoluminescence and optically stimulated luminescence responses of natural alexandrite. Applied Radiation and Isotopes 166, 109402. http://doi.org/10.1016/j.apradiso.2020.109402

Yukihara, E.G., 2020. A review on the OSL of BeO in light of recent discoveries: The missing piece of the puzzle? Radiation Measurements 134, 106291. http://doi.org/10.1016/j.radmeas.2020.106291

Instruments

Lim, K.T., Kim, H., 2021. Feasibility assessment of an SiPM for implementation in an OSL reader. Nuclear Instruments and Methods in Physics Research Section A: Accelerators, Spectrometers, Detectors and Associated Equipment 986, 164746. http://doi.org/10.1016/j.nima.2020.164746

Portable instruments

Castillo, M., Muñoz-Salinas, E., Sanderson, D.C.W., Cresswell, A., 2020. Landscape evolution of Punta Arena sand spit (SE Baja California Peninsula, NW Mexico): Implications of ENSO on landscape erosion rates. CATENA 193, 104601. http://doi.org/10.1016/j.catena.2020.104601

Muñoz-Salinas, E., Castillo, M., Franco-Ramos, O., Arce, J.L., Sanderson, D.C.W., Cresswell, A.C., 2020. Assessing paraglacial processes at Nexpayantla Gorge (Popocatépetl volcano, Central Mexico) using OSL and 14C. Earth Surface Processes and Landforms 45, 2450-2462. http://doi.org/10.1002/esp.4890

Munyikwa, K., Gilliland, K., Plumb, E., Gibson, T., 2020. Investigating post-depositional sediment mixing at an archaeological site on the northern Plains using a portable optically stimulated luminescence (OSL) reader. Journal of Archaeological Science: Reports 33, 102508. http://doi.org/10.1016/j.jasrep.2020.102508

Sanderson, D.C.W., Kinnaird, T.C., 2019. Optically stimulated luminescence dating as a geochronological tool for Late Quaternary sediments in the Red Sea region, in: Rasul, N.M.A., Stewart, I.C.F. (Eds.), Geological Setting, Palaeoenvironment and Archaeology of the Red Sea. Springer International Publishing, Cham, pp. 685-707. http://doi.org/10.1007/978-3-319-99408-6_31

Computer coding

Brown, N.D., 2020. Which geomorphic processes can be informed by luminescence measurements? Geomorphology 367, 107296. http://doi.org/10.1016/j.geomorph.2020.107296

Saha, S., Owen, L.A., Orr, E.N., Caffee, M.W., 2020. A statistical and numerical modeling approach for spatiotemporal reconstruction of glaciations in the Central Asian mountains. MethodsX 7, 100820. http://doi.org/10.1016/j.mex.2020.100820

Review

Duval, M., Arnold, L.J., Rixhon, G., 2020. Electron spin resonance (ESR) dating in Quaternary studies: evolution, recent advances and applications. Quaternary International 556, 1-10. http://doi.org/10.1016/j.quaint.2020.07.044

Falguères, C., 2020. The first human settlements out africa into Europe: A chronological perspective. Quaternary Science Reviews 247, 106551. http://doi.org/10.1016/j.quascirev.2020.106551

Falguères, C., 2020. A French story of the ESR dating method for Quaternary samples. Quaternary International 556, 11-19. http://doi.org/10.1016/j.quaint.2019.09.047

Grün, R., 2020. A very personal, 35 years long journey in ESR dating. Quaternary International 556, 20-37. http://doi.org/10.1016/j.quaint.2018.11.038

Guilarte, V., 2020. ESR dating in Archaeology, in: Shukla, A.K. (Ed.), Spectroscopic Techniques for Archaeological and Cultural Heritage Research. IOP Publishing, pp. 1-29. http://doi.org/10.1088/978-0-7503-2616-2ch2

Hornak, J.P., 2020. The development of low frequency EPR spectroscopy for studying objects with cultural heritage significance, in: Shukla, A.K. (Ed.), Spectroscopic Techniques for Archaeological and Cultural Heritage Research. IOP Publishing, pp. 1-60. http://doi.org/10.1088/978-0-7503-2616-2ch3

Moska, P., 2019. Luminescence dating of Quaternary sediments – some practical aspects. Studia Quaternaria 36, 161-169. http://doi.org/10.24425/sq.2019.126387

Toyoda, S., 2020. Determination by ESR of the temperature of prehistoric lithic heat treatment, in: Shukla, A.K. (Ed.), Spectroscopic Techniques for Archaeological and Cultural Heritage Research. IOP Publishing, pp. 1-13. http://doi.org/10.1088/978-0-7503-2616-2ch4

Yukihara, E.G., 2020. A review on the OSL of BeO in light of recent discoveries: The missing piece of the puzzle? Radiation Measurements 134, 106291. http://doi.org/10.1016/j.radmeas.2020.106291

Ancient TL

ISSN 2693-0935

Aims and Scope

Ancient TL is a journal devoted to Luminescence dating, Electron Spin Resonance (ESR) dating, and related techniques. It aims to publish papers dealing with experimental and theoretical results in this field, with a minimum of delay between submission and publication. Ancient TL also publishes a current bibliography, thesis abstracts, letters, and miscellaneous information, e.g., announcements for meetings.

Frequency

Two issues per annum in June and December

Submission of articles to Ancient TL

Ancient TL has a reviewing system in which direct dialogue is encouraged between reviewers and authors. For instructions to authors and information on how to submit to Ancient TL, please visit the website at:
http://ancienttl.org/TOC1.htm

Journal Enquiries

For enquiries please contact the editor:
Regina DeWitt, Department of Physics, East Carolina University, Howell Science Complex, 1000 E. 5th Street, Greenville, NC 27858, USA; Tel: +252-328-4980; Fax: +252-328-0753 (dewittr@ecu.edu)

Subscriptions to Ancient TL

Ancient TL Vol. 32 No.2 December 2014 was the last issue to be published in print. Past and current issues are available for download free of charge from the Ancient TL website:
http://ancienttl.org/TOC4.htm